Studiengang: Master of Science Biology

Masterarbeit:

Growth rates of *Desmophyllum dianthus* – Effect of association with endolithic algae

Vorgelegt von: Christiane Hassenrück

Betreuende Gutachterin: Carin Jantzen, PhD, Alfred Wegener Institute for Polar and Marine Research, Bremerhaven, Germany

Zweite Gutachterin: Prof. Gabriele Gerlach, PhD, Carl von Ossietzky Universität Oldenburg

Oldenburg, den

CONTENT

ABSTRACT

It has long been suggested that endolithic algae inside the skeleton of living corals might have a symbiotic relationship with the coral host and would positively affect coral calcification. However, so far this hypothesis has not yet been further explored. This study investigated the effect of endolithic algae on the growth performance of the cold-water coral *Desmophyllum dianthus* that is frequently associated with the endolithic chlorophyte *Ostreobium queckettii* and the cyanobacterium *Plectonema terebrans*. The fluorescent staining agent calcein was used to document the upward and inward linear growth of septa of specimens of *D. dianthus* at Fjord Comau, southern Chile. Further qualitative observations concerned skeletal microstructure and density using light field and fluorescence microscopy and x-ray computed tomography, respectively. Since the *D. dianthus* was sampled in a region displaying strong annual fluctuations of environmental parameters that might influence calcification, growth rates were also tested for a seasonal pattern. The results of this study show a severe reduction of growth rates associated with endolithic algae. Infested individuals grew about half as fast as non-infested polyps referring to both directions of septal growth with median values of 1.18μm/day for upward and 0.49μm/day for inward growth compared to 2.76μm/day and 0.82μm/day, respectively. These results point towards a parasitic relationship between *D. dianthus* and its endolithic algae refuting the hypothesis of a mutually beneficial association. This theory is further supported by observations on skeletal density and microstructure which suggest a reduction in skeletal density probably caused by extensive tunnelings of both endolithic species. Unlike expected the seasonal variation of upward septal growth rates of *D. dianthus* was inconsistent with the annual temperature pattern at Fjord Comau. Minimum growth rates were reported in periods of maximum temperatures – a phenomenon that might be explained by the trade-off between growth and reproduction which is suspected to take place in summer. Inward growth rates displayed a continuous decrease with time that is most likely attributed to the increasing influence of morphological constraints towards the center of the polyp. Although this study appears to conclusively indicate a negative effect of the association of *D. dianthus* with endolithic algae, controversial evidence has been discovered regarding metabolic links between the coral host and the endoliths and further research is necessary to fully resolve the issue.

1. INTRODUCTION

1.1 Coral calcification and the phenomenon of light-enhanced calcification

Scleractinian coral polyps are the engineers of extensive reefs and coral banks in tropical as well as cold water regions. The key process of the formation of such structures is the deposition of the calcareous aragonite skeleton by the coral polyp – a process known as calcification. Coral calcification has been studied for over 150 years providing a comprehensive view of the matter.

The basic chemistry of calcification is the conversion of dissolved inorganic carbon and ionic calcium to calcium carbonate crystals (Allemand et al., 2004; Tambutté et al., 2011). This reaction is mediated by the basal part of the outer cell layer of the coral polyp, the Calicoderm (Allemand et al., 2011). Calcium carbonate does not precipitate spontaneously in seawater (Pytkowicz, 1973). However, the chemical properties of the medium in the area between the coral skeleton and the Calicoderm, referred to as subcalicoblastic extracellular calcifying medium, are modified by the coral polyp to allow for calcification (Al-Horani et al., 2003; Allemand et al., 2011; Tambutté et al., 2011). The subcalicoblastic extracellular calcifying medium is also characterized by a matrix of organic material, mostly proteoglycans, which is associated with a catalytic activity and influences the direction of crystal growth (Cuif and Dauphin, 2005a; Tambutté et al., 2006). These mechanisms to facilitate calcification pose high energy requirements to the calicoblastic cells which contain a large number of mitochondria (Allemand et al., 2004, 2011).

The ultrastructure of coral skeletons shows a distinct pattern of aragonite crystal formation (Stolarski, 2003; Cuif and Dauphin, 2005a). Two structural units can be identified: Centers of Rapid Accretion also called early mineralization zones and Thickening Deposits (Stolarski, 2003; Cuif and Dauphin, 2005a; Nothdurft and Webb, 2006). Centers of Rapid Accretion are thereby characterized by a high content of organic material and build the framework for the precipitation of thickening deposits (Cuif and Dauphin, 1998, 2005a; Stolarski, 2003). The formation of Centers of Rapid Accretion as well as thickening deposits is assumed to be strongly biologically controlled relying on the superposition of organic compounds by skeletal fibers (Cuif and Dauphin, 2005b). In the septa of coral skeletons Centers of Rapid Accretion are arranged in a rapid accretion front

mediating upward septal growth, whereas thickening deposits account for the lateral growth of septa (Stolarski, 2003; Cuif and Dauphin, 2005a).

In tropical corals the rate of calcification is enhanced by the photosynthetic activity of zooxanthellae (Gattuso et al., 1999). Several mechanisms of how photosynthesis and calcification might be linked have been proposed since the discovery of the phenomenon of light-enhanced calcification in the 1930s (Yonge, 1931; Yonge and Nicholls, 1931). Most explanations focus on the lesser amount of energy required for calcification when linked to photosynthesis (Chalker and Taylor, 1975; McConnaughey and Whelan, 1997; Furla et al., 2000; Al-Horani et al., 2003; Moya et al., 2006).
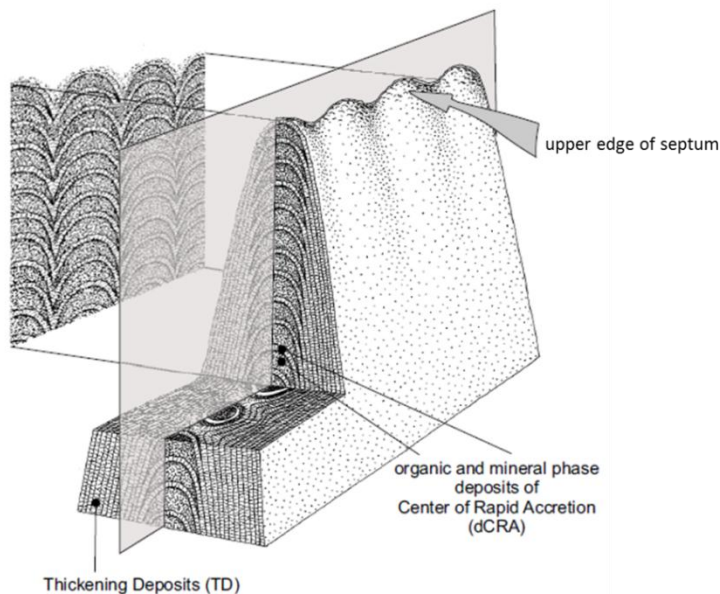
Figure 1: Three−dimensional model of septal microstructure showing perfect continuity between organo−mineral phases of dRAF and TD regions; real coral specimens usually have some regions with dRAF and TD layers continuing, and some parts where these layers discontinue; modified after Stolarski (2003).

1.2 Endolithic communities in scleractinian corals

Unlike tropical corals, scleractinians in cold or deep-water systems do not contain endosymbiotic algae that might promote calcification (Buhl-Mortensen and Mortensen, 2004). However, zooxanthellae are not the only phototrophic microorganisms closely associated with living coral polyps. Endolithic algae are common in coral skeletons of

corals in tropical as well as temperate and cold-water regions (Highsmith, 1981; Le Campion-Alsumard et al., 1995; Schlichter et al., 1997; Försterra et al., 2005). The coral skeleton provides a three-dimensional environment reducing the competition for space and offers protection from wave action, fluctuation in environmental parameters, UV radiation and grazers making it preferable to conditions on the outside (Shashar et al., 1997; Försterra et al., 2005; Rotjan and Lewis, 2005). The most common endolithic algae in living coral skeletons are the filamentous chlorophyte *Ostreobium queckettii* (Bornet and Flahault, 1889) and the cyanobacterium *Plectonema terebrans* Bornet and Flahault, 1889 (Le Campion-Alsumard et al., 1995; Tribollet, 2008; figure 2). They are low-light specialists and adapted to decreased light intensities and different spectral composition inside a coral skeleton (Fork and Larkum, 1989; Shashar and Stambler, 1992; Schlichter et al., 1997; Carreiro-Silva et al., 2009).

Unlike heterotrophic endolithic microorganisms that are usually associated with a negative impact on their coral host, positives effects have long been suggested to originate from the infestation with phototropic endoliths (Odum and Odum, 1955; Tribollet, 2008). Similar to the symbiosis with zooxanthellae in tropical corals, endolithic algae are suspected to supply nutrients to their coral host and promote calcification (Odum and Odum, 1955). Evidence for this hypothesis has been found in bleached specimens of *Oculina patagonica* (Fine and Loya, 2002) and in the azooxanthellate Mediterranean species *Tubastrea micranthus* (Schlichter et al., 1995) where photoassimilates were transferred from the endolith to the coral host in both cases. However, there is no indication of a significant contribution to the metabolism of healthy zooxanthellate corals (Kanwisher and Wainwright, 1967; Shashar and Stambler, 1992; Schlichter et al., 1997). The influence of endolithic algae on calcification has not yet been characterized apart from one study that reported *O. queckettii* to have no effect on the skeletal integrity of tropical corals (Highsmith, 1981). Furthermore, there has been no research on the effect of endolithic algae on calcification in azooxanthellate corals.
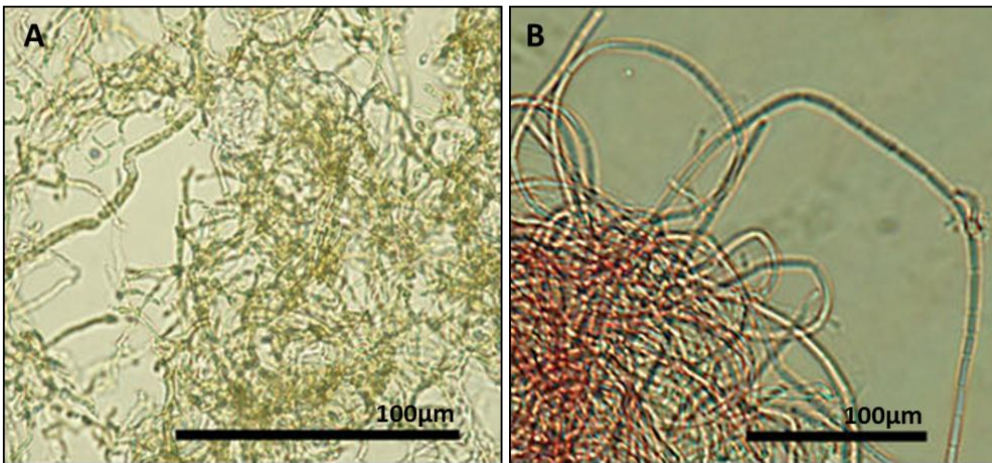
Figure 2: Filaments of *O. queckettii* (A) and *P. terebrans* (B) isolated from skeletons of *D. dianthus*; modified after Försterra and Häussermann (2008).

1.3 Ecology of *Desmophyllum dianthus* in Patagonia, Chile

Desmophyllum dianthus (Esper, 1794) is a cosmopolitan azooxanthellate cold-water coral (Försterra et al., 2005; Miller et al., 2011, figure 3). In southern Chile *D. dianthus* is the most abundant scleractinian known to reach densities of more than 1500 individuals per m² (Försterra and Häussermann, 2003; Cairns et al., 2005). It is commonly found in depths between 20 and 2460m but has been encountered as shallow as 7m (Försterra and Häussermann, 2003; Cairns et al., 2005). *D. dianthus* is a solitary species that forms pseudocolonies by settling on skeletons of its own species (Försterra and Häussermann, 2003; Miller et al., 2011); figure 3E). Its preferred habitat are rocky overhangs exposed to moderate currents where it grows downwards presumably to avoid sedimentation (Försterra and Häussermann, 2003; Cairns et al., 2005; Försterra et al., 2005). Growth rate estimates range from 0.5 to 2.3 mm per year (Risk et al., 2002; Försterra and Häussermann, 2003; Adkins et al., 2004). As it grows the tissue retracts from the lower areas of the skeleton leaving them accessible to boring organisms that in time compromise the structural integrity of the skeleton (Lazier et al., 1999; Försterra and Häussermann, 2003). This process leads to the detachment and subsequent death of the coral polyp (Försterra and Häussermann, 2003; Thresher et al., 2011). It limits the life expectancy of *D. dianthus* which is estimated at a maximum of about 190 years (Thresher et al., 2011).

The shallow-water occurrence of *D. dianthus* in depths where light can still penetrate makes skeletons of this species a suitable host for phototrophic endoliths (Försterra and Häussermann, 2003; Cairns et al., 2005). In southern Chile specimens of *D. dianthus* are infested by two species: *O. queckettii* and *P. terebrans* (Försterra et al., 2005; figure 3C and D). The endoliths gain access after the retraction of the tissue from the lower skeleton (Lazier et al., 1999; Försterra and Häussermann, 2008). They inhabit the outer layers of the skeleton in areas where it is covered by tissue (Försterra et al., 2005; Försterra and Häussermann, 2008). Infestation with these two endolithic species is not mutually exclusive although the majority of infested polyps only harbor *O. queckettii* (Försterra and Häussermann, 2008). *P. terebrans* is less common and usually restricted to the light-exposed side of the coral polyp (Cairns et al., 2005; Försterra et al., 2005; Försterra and Häussermann, 2008). A previous study conducted at Fjord Comau in southern Chile estimated the total number of infested shallow-water *D. dianthus* at 83% (Försterra and Häussermann, 2008).

1.4 Potential symbiosis between endolithic algae and *D. dianthus*

The close association of the endolithic algae and their host *D. dianthus* has led to the hypothesis that this relationship may be mutually beneficial (Cairns et al., 2005; Försterra et al., 2005; Försterra and Häussermann, 2008). Judging by the exclusive occurrence of endolithic algae in skeletal areas that are covered by tissue, the spatial proximity may be initiated by both organisms to gain mutual advantages (Försterra et al., 2005). The exchange of nutrients between the algae and the surrounding seawater is mediated by the coral tissue (Försterra and Häussermann, 2008). This may hint at a mutual transfer of substances to benefit the endolith and the coral polyp (Försterra and Häussermann, 2008). Furthermore, infested areas of the coral skeleton appear to have thicker thecae indicating an effect on calcification (Försterra et al., 2005). However, this study only examined two partially infested individuals of D. dianthus (Försterra et al., 2005). Based on the above observations, Försterra et al. (2005) and Försterra and Häussermann (2008) suggested a symbiosis between *D. dianthus* and its endolithic algae.
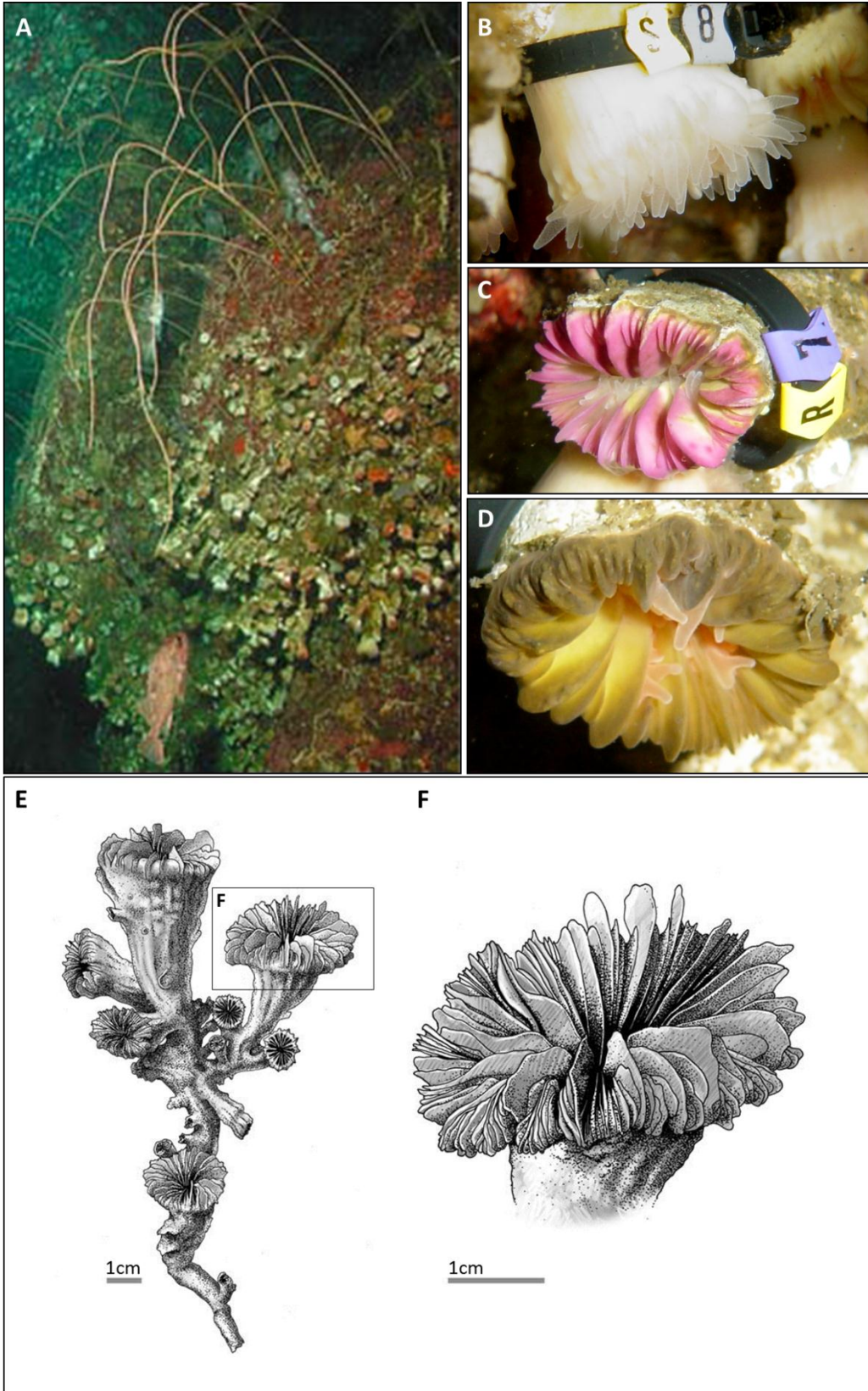
Figure 3: *D. dianthus*, A: coral bank of *D. dianthus*, Fjord Comau, Southern Chile, modified after Försterra et al. (2005), B: non-infested polyp, C: polyp infested with *P. terebrans* and to a lesser degree *O. queckettii*, D: polyp infested with *O. queckettii*, E: schematic of a pseudocolony of *D. dianthus* and an individual polyp (F), modified after Roberts et al. (2009).

So far, no coral-algal symbioses in cold-water corals have been documented (Buhl-Mortensen and Mortensen, 2004) and although a mutualistic relationship has been suggested for *D. dianthus* and its endolithic algae, no evidence is available on the matter. I hypothesize that a symbiosis would positively affect skeletal growth rates of *D. dianthus* similar to light-enhanced calcification in tropical corals. To test this hypothesis the linear extension of septa of algae-infested and non-infested individuals of *D. dianthus* was measured. Between January and December 2006 specimens of *D. dianthus* at Fjord Comau, southern Chile, were stained in-situ every four months with the fluorescent agent calcein to mark growth periods. This technique has been proven to be a reliable tool to document growth of calcifying organisms (Rowley and Mackinnon, 1995; Marschal et al., 2004; Brahmi et al., 2009; Tambutte et al., 2011). Coral polyps were harvested for sclerology in 2007 five to ten months after the last staining event. Measurements involved the inward and upward linear extension of septa. Growth rates were compared between infested and non-infested individuals as well as among different sampling sites. Since Patagonia is a region with pronounced seasonality of environmental parameters such as temperature that might influence calcification rates (Weber et al., 1975; Lazier et al., 1999; Marshall and Clode, 2004), the effect of growth period was included in the analysis. Additionally, skeletal microstructure was compared between infested and non-infested polyps of *D. dianthus*.

2. METHODS

2.1 Sampling area

D. dianthus was sampled at five different sites along the Fjord Comau in southern Chile between 42.41° and 42.15° latitude. The sampling sites were designated as Punta Huinay (PH), across Punta Huinay (XH), Punta Gruesa (PG), a steep wall after Punta Llonco (SW) and Liliguapi (LI). Four of these five sampling sites were located in close proximity well within the fjord (mid-fjord sites), whereas the fifth site was at the mouth of the fjord on Isla Liliguapi (outer fjord) adjacent to the Gulf of Ancud (figure 4).

Fjord Comau is part of the Chilean fjord system that spans more than 1500km between 42° and 55° latitude (Försterra et al., 2005). The fjord extends about 41km into the main land and has a maximum depth of approx. 500m (Pickard, 1971; Endesa Fundacion San Ignacio del Huinay). It is characterized by steep walls and wide but shallower mouth compared to the rest of the fjord (Endesa Fundacion San Ignacio del Huinay). Tidal ranges of up to 7m with moderate tidal currents have been reported at Fjord Comau (Endesa Fundacion San Ignacio del Huinay). High precipitation, especially in winter, and freshwater run-off from rivers and glaciers are creating a superficial layer of low salinity that is characteristic of fjords in this region (Pickard, 1971). At Fjord Comau temperature and salinity of this surface layer vary between 12 - 22°C and 7 - 31‰, respectively (Försterra and Häussermann, 2003). The presence of such a surface layer is documented for the whole length of the fjord decreasing in thickness only at its mouth (Iriarte et al., 2007). The water masses below offer more stable conditions with temperature and salinity ranging from 8 to 13.5°C and 28.5 to 34‰, respectively and host extensive coral banks of *D. dianthus* (Försterra and Häussermann, 2003; Cairns et al., 2005).
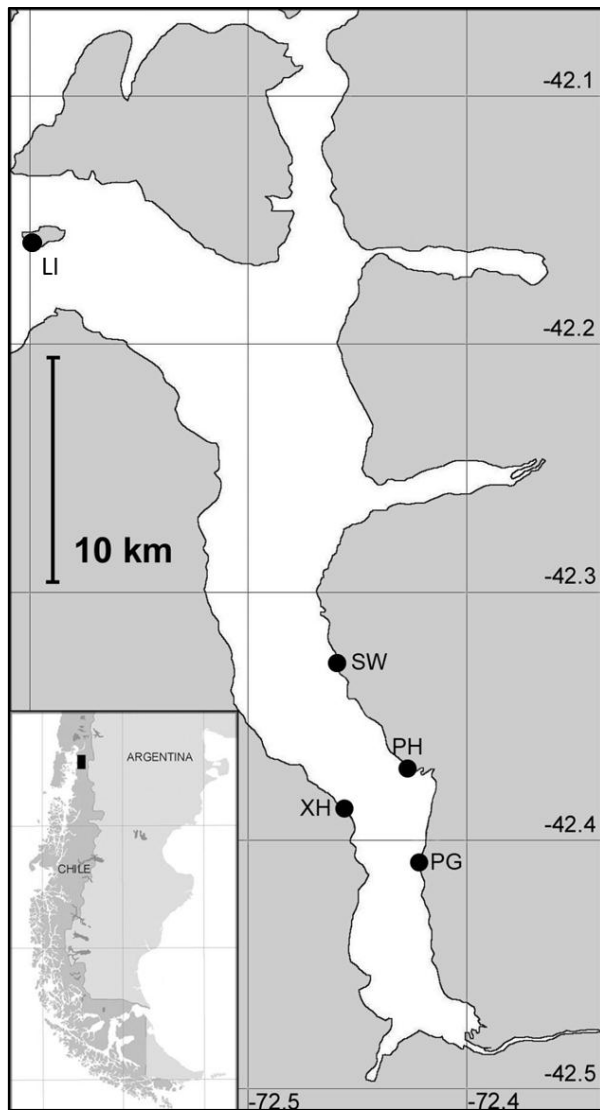
Figure 4: Map of sampling sites at Fjord Comau, southern Chile; PH: Punta Huinay, XH: across Punta Huinay, PG: Punta Gruesa, LI: Isla Liliguapi, SW: steep wall after Punta Llonco.

2.2 Staining

Seven to fourteen algae-infested and non-infested polyps of *D. dianthus* were selected, tagged and photographed at each site in 14-22m actual depth via SCUBA diving. Specimens were similar in size to minimize the influence of an age bias on data analysis. Coral polyps were stained every four months in January, April, August and December 2006. At each staining event specimens were exposed to a 500mg/l calcein solution for 16 to 24h. The staining agent was applied in-situ by fitting a small plastic bag around the coral polyp and injecting the staining agent into the bag. Successfully stained polyps emitted a

faint greenish glow after the removal of the bag (figure 5). In May till October 2007 the polyps were harvested and afterwards conserved in Ethanol, 96%.
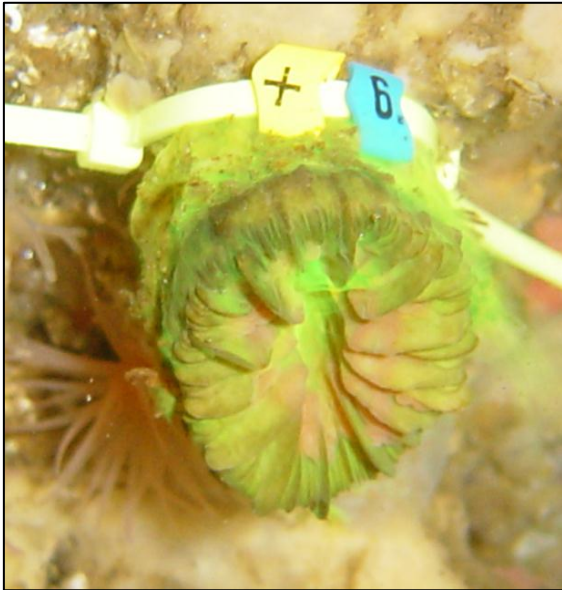
Figure 5: Freshly stained individual of *D.dianthus* infested with endolithic algae at Isla Liliguapi.

2.3 Sclerology

The top 2cm of each polyp of *D. dianthus* were cut off and embedded in two component epoxy resin. Prior to embedding the coral polyps were air-dried for 48h to remove all Ethanol which was essential to ensure a solid consistency of the epoxy resin. Two different kinds of two component epoxy resin were employed to embed the samples of *D. dianthus*: epoxy 300 with the corresponding hardener 3100 and araldite 2020. Samples embedded in epoxy 300 were cured for 48h under room conditions whereas samples embedded in araldite 2020 were exposed to a pressure of approx. 5bar for 24h. In both cases the tiny air bubbles stuck between the septa of a polyp could not be completely eliminated, slightly compromising the integrity of the embedded specimen during sectioning.

Of each coral polyp four sections were cut with a low speed diamond saw: two longitudinal sections at the highest point of upward septal extension and two transversal sections about 4mm below the upper edge of the theca (figure 6A). Each section was

between 0.7 and 1mm thick and ground to approx. 0.01mm with grinding paper of grain sizes 15μm and 10μm. For the three dimensional reconstruction of fluorescent microscopy images another grinding step with a grain size of 5μm was added.

The inward (transversal sections) and upward (longitudinal sections) extension of septa were measured using a fluorescence high power microscope (model: Zeiss Axioskop) and a stereomicroscope (model: Olympus SZX12) with an excitation wavelength of 450 to 490nm. Images and measurements were taken with a camera (model: Olympus DP70 and DP72, respectively) and corresponding software. Ideally, each staining event was marked with a cone-shaped fluorescent growth band at the tip of a septum (figure 6B). Measurements were taken from tip to tip of such growth bands. Whenever the number of growth bands did not correspond to the number of staining events or when the growth bands were not clearly distinguishable from each other, the septum was not measured. If less than five septa had been measured per section, additional sections were prepared where possible. For each polyp an average growth of the upward as well as inward septal extension was calculated by taking the mean of all measured septa (equation 1). Daily growth rates were then calculated by dividing average septal extension per polyp by the number of days between staining events (equation 2).

$$average\ extension\ of\ septa[\text{μ}m] = \frac{\sum(measurement\ per\ septum\ [\text{μ}m])}{number\ of\ measured\ septa} \qquad (1)$$

$$daily\ growth\ rate\ [\text{μ}m/day] = \frac{average\ extension\ of\ septa\ [\text{μ}m]}{length\ of\ growth\ period\ [day]} \qquad (2)$$
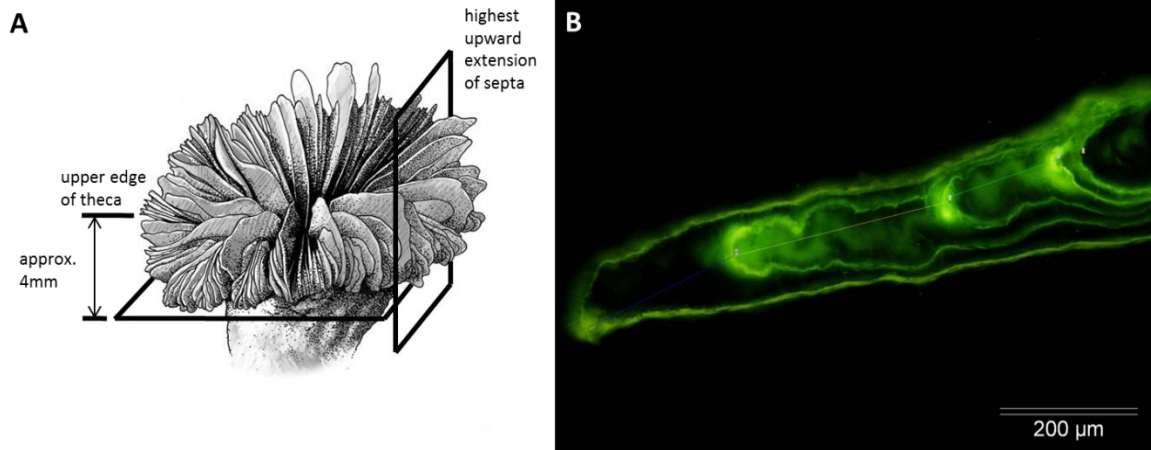
14

Figure 6A: Schematic of a polyp of *D. dianthus* depicting the orientation of the cutting planes for the sclerological sections to measure septal growth; modified after Roberts et al. (2009); B: longitudinal section of a septum with four distinct growth bands (green), measurements in red (Jan '06 – Apr '06), green (Apr '06 – Aug '06), yellow (Aug '06 – Dec '06) and blue (Dec '06 – 2007), polyp sampled at a steep wall after Punta Llonco, Fjord Comau, southern Chile.

2.4 Statistical analysis

To meet the assumption of normally distributed data septal growth rates were ln-transformed when parametric tests were applied. However, the graphical representation of the data is given without this transformation.

A preliminary analysis to account for the possibility of a sampling bias in polyp size was conducted. The polyp diameter was measured and compared between infested and non-infested polyps and among sites with a two-way ANOVA. Additionally, it was correlated with the ln-transformed growth rates of infested as well as non-infested polyps using Pearson's coefficient of correlation (table 1). Values are given as mean diameter ± standard error.

The comparison of daily growth rates to identify the effect of endolithic algae on calcification was divided into two separate analyses: (I) the comparison of septal growth rates using mean values of all four growth periods and (II) the analysis of seasonal changes in septal growth rates. The first analysis compared upward and inward growth rates of infested and non-infested individuals from all five sites using an independent sample t-test. This analysis was extended to consider differences between outer fjord and mid-fjord sites as well. In this context the data on septal growth rates from PG, PH, SW and HX was

pooled and compared to septal growth at Isla Liliguapi. Differences were tested between infested and non-infested polyps at each location and between outer and mid-fjord sites for infested and non-infested polyps separately using independent-sample t-tests. Welch's modification was applied in case of heterogeneous variances. Significance levels were bonferroni-adjusted at α=0.013. This approach was chosen although the experiment was originally designed for a two-way ANOVA with the factors infestation and site. However, the highly heterogeneous data on inward septal growth rates did not meet the assumptions of the ANOVA model. Upward septal growth rates were mathematically qualified for the ANOVA design.

For the second analysis growth periods were defined from January '06 to April '06, April '06 to August '06, August '06 to December '06 and from December '06 to the coral harvest in 2007. Polyps that were not found at each staining event and therefore displayed less than the regular four growth bands were excluded from the analysis. Growth between two consecutive calcein bands then spanned more than two growth periods and could not be attributed to either one in particular. A repeated measurements MANOVA was conducted to determine differences in septal growth rates between infested and non-infested polyps as well as between growth periods. The factor site was not considered. To test for differences in growth rates between consecutive growth periods, paired-sample t-tests were run as planned comparisons on infested as well as non-infested individuals for both directions of septal growth (table 1).

Given the small sample size of this experiment, algal infestation has been treated as a factor with two levels, although growth rates might also be proportionally affected by the severity of infestation. To include this information in the analysis growth rates were correlated with the percentage surface area of the polyp colored by the presence of endolithic algae using a Spearman's rank correlation (table 1). Non-transformed data was used in this analysis.

All analyses were conducted in PASW 18 except for the repeated measurements analysis and Spearman's rank correlation that were done in STATISTICA 10. Detailed results of the statistical tests are included in appendix B. Values in the text are given as median growth rates of non-transformed data.

Table 1: Summary of the statistical analysis of septal growth rates of *D. dianthus* at Fjord Comau, southern Chile; septal growth rates ln-transformed except for the correlation with the degree of infestation; in italics: additional analysis of unward septal growth rates (results displayed in appendix B).

Analysis	Test (Model)
Differences in polyp diameter	Two-way ANOVA Diameter ~ infestation + site + infestation*site
Correlation between growth rates and polyp size	Pearson's correlation
Differences in septal growth rates	Independent-sample t-test
Differences along the length of Fjord Comau	Independent-sample t-test (bonferroni-adjusted α=0.013)
Differences in upward growth rates	*Two-way ANOVA* *Upward growth rates ~ infestation + site + infestation*site*
Seasonal variability of septal growth rates	RM-MANOVA Univariate effects: Inward growth rates ~ infestation Multivariate effects: Inward growth rates ~ growth period + infestation *growth period
Planned comparisons between consecutive growth periods	Paired-sample t-test
Correlation of septal growth rates and the degree of infestation	Spearman's rank correlation

2.5 Three-dimensional reconstruction

Two different approaches were chosen for the three dimensional reconstruction of *D. dianthus*: (I) the stacking of fluorescent microscopy (FM) images and (II) X-ray computed tomography. Two stained specimens were selected for the first technique: one infested polyp from Punta Gruesa and one non-infested individual from across Punta Huinay. Transversal sections were cut every 0.8mm and ground as described in chapter 2.3 Sclerology. Accounting for the thickness of the saw blade (0.4mm) this resulted in one

image every 1.2mm. Pictures were taken under a fluorescence stereomicroscope (model: Olympus SZX12) with a camera (model: Olympus DP72). Several images were taken of each section since the lowest magnification of the fluorescence microscope did not allow for only one image being taken of the whole section. These images were processed in Microsoft Image Composite Editor to form one image per section. Stacking of fluorescence microscopy images and three-dimensional rendering were attempted in AMIRA 5.4.1. Additional to the three-dimensional reconstruction, two-dimensional images of selected infested and non-infested polyps were compared to describe differences in skeletal characteristics between infested and non-infested individuals as well as between polyps infested exclusively with *O. quecketti* and *P. terebrans*. Pictures were taken under a high power microscope (model: Zeiss Axioskop) with a camera (model: DP70) and included fluorescence as well as light field microscopy images.

Four coral polyps were selected for the CT-analysis. These polyps were not part of the original number of stained individuals but chosen from additionally harvested polyps in close proximity to stained polyps. Three of these four polyps were collected at across Punta Huinay (one infested and two non-infested individuals) and another infested polyp at Punta Gruesa. Air-dried polyps were scanned with a spiral CT (AWI-ICE CT; Freitag, 2012, pers. comm.) at an x-ray voltage of 140kV and a target current of 200μA. X-ray images had a resolution of 56μm per pixel and were stacked one image every 100μm. Image stacks were processed in AMIRA 5.4.1 for volume rendering. Different grey-scale values of pixels of X-ray images further allowed for an assessment of differences in skeletal density (Bosscher, 1993) between algae infested and non-infested polyps.

3. RESULTS

3.1 Sample sizes

During the experiment the sample sizes for the analysis of growth rates in *D. dianthus* were severely reduced. Out of the original 104 polyps that were tagged at Fjord Comau only 66 could be recovered in 2007 at the coral harvest. Of these individuals 42 polyps were provided for this study already embedded in epoxy resin (Willenz, 2011, pers. comm.). 19 polyps of these 42 were processed in a way that did not allow for sclerological analysis mostly because of an insufficiently solid consistency of the embedding resin. A total of 47 polyps, representing roughly 45% of the originally tagged individuals, remained for the analysis of growth rates, of which 25 were infested by endolithic algae. Most of the infested polyps showed a green coloring by *O. queckettii*. Four individuals were infested by both endolithic species and another four exclusively by *P. terebrans*. Of the 47 polyps used for the sclerological analysis some could only be used for upward and not inward measurements of septa and vice versa. This sample size was further reduced for the analysis of the seasonal variability of growth rates due to the exclusion of polyps with less than four growth bands. In case of Punta Huinay this reduction resulted in a sample size of only one infested and one non-infested individual (table 2).

Table 2: Final sample sizes of the analysis of septal growth rates of *D. dianthus* at Fjord Comau, southern Chile; LI: Isla Liliguapi, PG: Punta Gruesa, PH: Punta Huinay, SW: steep wall after Punta Llonco, XH: across Punta Huinay.

		Mean growth rates		Seasonal variability	
		non-infested	infested	non-infested	infested
Upward growth		**21**	**23**	**19**	**15**
	LI	6	5	6	4
	PG	4	3	4	3
	PH	3	3	1	1
	SW	3	8	3	5
	XH	5	4	5	2
Inward growth		**22**	**24**	**20**	**17**
	LI	6	5	6	4
	PG	4	4	4	4
	PH	3	3	1	1
	SW	3	9	3	6
	XH	6	3	6	2

Specimens of *D. dianthus* at Fjord Comau, southern Chile were young adults with diameters ranging from 12.11mm ± 0.85 of non-infested polyps at Punta Gruesa to 20.82mm ± 0.76 of infested polyps at Isla Liliguapi. In general infested polyps were larger with a diameter of 17.97mm ± 0.37 than non-infested individuals with 15.04mm ± 0.39 (p<0.001). Regardless of infestation, the size of *D. dianthus* also varied among sites (p<0.001). However, the effect of infestation depended on site as indicated by a significant interaction of these two factors (p=0.031). The largest differences in mean diameter were found at LI, PG and PH where infested polyps were approx. 20 to 40% larger than non-infested ones. At SW and XH this difference was only marginal (figure 7).

To exclude an influence of polyp size on growth rates, polyp diameter was correlated with ln-transformed upward and inward septal growth rates (USGR and ISGR, respectively). Correlations proved to be insignificant for infested polyps. Non-infested polyps showed a weak but significant positive correlation of polyp diameter and septal growth rates (USGR: R=0.445, p=0.049; ISGR: R=0.626, p=0.002). Regarding septal growth during different growth periods, significant correlations were restricted to the ISGR of non-infested polyps between January and April 2006 (R=0.585, p=0.011) and August to December 2006 (R=0.575, p=0.010). In all significant cases septal growth rates increased with polyp size.

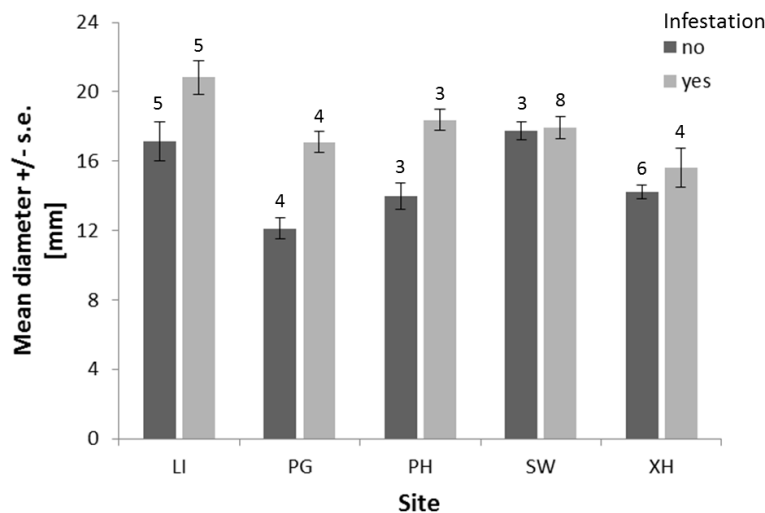Detailed results on the ANOVA and all correlations are given in appendix B, tables 9 and 10, respectively.

Figure 7: Mean diameter ± standard error (s.e.) of *D. dianthus* at five sites at Fjord Comau, southern Chile; numbers above bars indicating sample size; LI: Isla Liliguapi, PG: Punta Gruesa, PH: Punta Huinay, SW: steep wall after Punta Llonco, XH: across Punta Huinay.

3.3 Growth rates averaged over all growth periods

Upward as well as inward septal growth rates were significantly higher in non-infested polyps of *D. dianthus* (USGR: p<0.001; ISGR: p=0.017). Non-infested polyps grew approx. twice as fast with 2.76µm/day (USGR) and 0.82µm/day (ISGR) than infested individuals with 1.18µm/day and 0.49µm/day, respectively.

Comparison between infested and non-infested individuals at outer and mid-fjord sites

Including the location along the course of the fjord in the above comparison, USGR and ISGR of infested and non-infested individuals only differed significantly at Isla Liliguapi as opposed to growth rates at mid-fjord sites (table 3). USGR of non-infested polyps at Isla Liliguapi were almost 30 times higher than growth rates of infested individuals (9.12µm/day and 0.31µm/day, respectively; figure 8A). ISGR at Isla Liliguapi differed by a factor of approx. five between non-infested individuals (1.63µm/day) and infested polyps (0.34µm/day; figure 8B). At the mid-fjord sites septal growth rates of non-infested individuals were only slightly higher than those of infested polyps. USGR of 1.22µm/day (infested) and 2.19µm/day (non-infested) were recorded at mid-fjord-sites (figure 8A), as well as ISGR of 0.59µm/day (infested) and 0.67µm/day (non-infested; figure 8B). However, these differences were not significant (table 3).

Comparison between outer and mid-fjord sites of infested and non-infested polyps

The comparison between outer and mid-fjord sites revealed a significant difference in septal growth rates of non-infested polyps (table 3). USGR of non-infested polyps at Isla Liliguapi (9.12µm/day) were more than four times as high as at the mid-fjord sites (2.12µm/day; figure 8A). ISGR of non-infested polyps at Isla Liliguapi (1.63µm/day) were approx. 2.5 times higher compared to 0.67µm/day at the mid-fjord sites (figure 8B). Growth rates of infested polyps did not differ significantly between outer and mid-fjord sites (table 3), although slightly smaller growth rates were recorded at Isla Liliguapi. USGR of 0.31µm/day were measured at Isla Liliguapi compared to 1.22µm/day at mid-fjord sites (figure 8A). ISGR showed values of 0.34µm/day at Isla Liliguapi and 0.59µm/day at the mid-fjord sites (figure 8B).

Table 3: Results of the comparison of septal growth rates of *D. dianthus* at Fjord Comau, southern Chile, between infested and non-infested polyps accounting for differences between outer and mid-fjord sites (outer fjord: Isla Liliguapi, mid-fjord: pooled data from PG, PH, SW and XH); independent-sample t-tests at a bonferroni-adjusted significance level of α=0.013; significant results in bold script; tests conducted on ln-transformed growth rates.

	Upward growth of septa			Inward growth of septa		
	t	df	p	t	df	P
Infested vs. non-infested						
Outer fjord	**-5.129**	**4.434**	**0.005**	**-5.381**	**9**	**<0.001**
Mid-fjord	-2.135	27.629	0.042	-0.537	26.284	0.596
Outer fjord vs. mid-fjord						
Infested	-1.243	21	0.228	-1.857	22	0.077
Non-infested	**4.990**	**19**	**<0.001**	**5.251**	**20**	**<0.001**

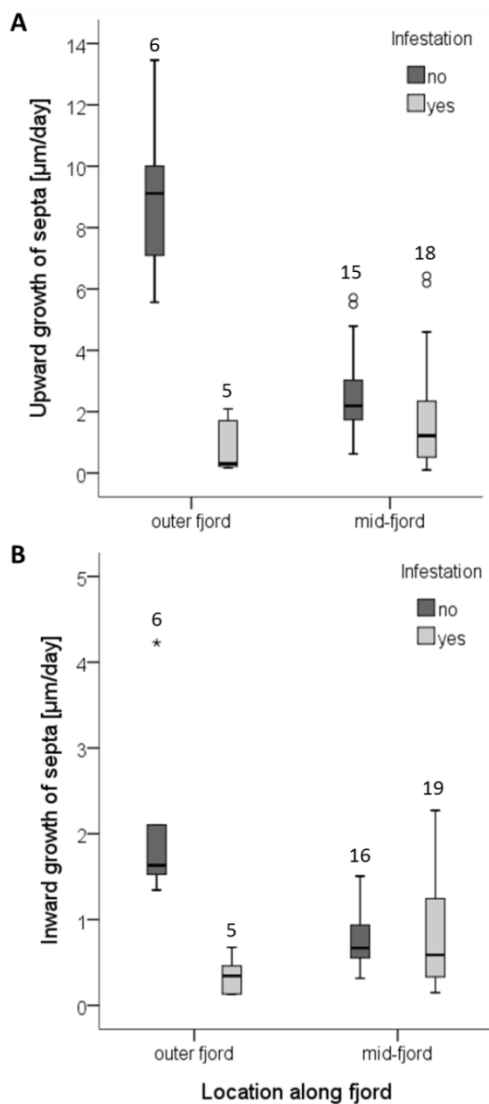Figure 8: Growth rates of *D. dianthus* at Fjord Comau, southern Chile; A: upward growth of septa; B: inward growth of septa; numbers above boxplots indicating sample size; boxplot depicting median, interquartile range and non-outlier minimum and maximum, empty circles: mild outliers (more than 1.5 times the interquartile range), asterisks: extreme outliers (more than 3 times the interquartile range).

3.4 Seasonal variability of growth rates

The analysis of seasonal variability in septal growth rates of *D. dianthus* revealed a significant effect of growth period (USGR: p<0.001; ISGR: p<0.001). Furthermore, the main effect of infestation was confirmed for both directions of septal growth with infested polyps growing considerably slower (USGR: p<0.001; ISGR: p<0.014). Detailed results on the RM-MANOVAs are given in appendix B, table 11. USGR between December 2006 and the coral harvest in May to October 2007 corresponded roughly to mean values of the first two growth periods in 2006 (figure 9A). This pattern was not observed in ISGR (figure 9B).

Seasonal pattern of USGR

USGR of non-infested polyps display a continuous increase from the seasonal minimum of 1.15µm/day in January to April 2006 to a peak in August to December 2006 with 4.30µm/day almost four times as high as the seasonal minimum (figure 9A). Differences in USGR of non-infested polyps between consecutive growth periods were significant in all cases (table 4). A similar but less pronounced pattern was observed in the USGR of infested polyps. The peak in August to September 2006 was less than twice as high with 0.76µm/day compared to minimum values in January to April 2006 and April to August 2006 of 0.47µm/day and 0.41µm/day, respectively (figure 9A). Unlike the USGR of non-infested polyps, infested individuals did not display significant differences between consecutive growth periods with the exception of the last to growth periods (table 4). The effect of infestation ranged from an approx. three-fold difference in USGR between infested and non-infested polyps in January to April 2006 to more than 5.5-fold difference in August to December 2006 (figure 9A).

Seasonal pattern of ISGR

Inward growth rates displayed a distinctively different pattern. Non-infested polyps grew fastest within the first months of the experiment with continuously decreasing growth rates during the following months. Although ISGR of non-infested polyps were slightly smaller in January to April 2006 (0.95µm/day) compared to the second growth period (1.03µm/day), the first four months were characterized by a wider range towards higher

values. From the second to the last growth period ISGR of non-infested polyps declined by approx. 35% with each measurement to a minimum value of 0.38µm/day during the last growth period (figure 9B). Planned pairwise comparisons showed that the decrease in growth rates between consecutive growth periods was significant (table 4). ISGR of infested polyps displayed no apparent seasonal pattern of growth rates. Median values varied between 0.32µm/day in August to December 2006 and 0.49µm/day in December 2006 to 2007 (figure 9B). Planned comparisons could not detect any significant differences between growth periods (table 4). This change in the effect of seasonality on ISGR between infested and non-infested polyps was further emphasized by a significant interaction of the two factors ($p = 0.002$).

Table 4: Planned pairwise comparisons on the analysis of the seasonality of septal growth rates of *D. dianthus* at Fjord Comau, southern Chile, using paired-sample t-tests; significant results in bold script; tests conducted on ln-transformed growth rates.

| Growth periods	Non-infested			Infested		
	t	df	p	t	df	p
Upward growth						
Jan '06 – Apr '06 vs. Apr '06 – Aug '06	**-3.847**	**15**	**0.002**	-0.715	13	0.487
Apr '06 – Aug '06 vs. Aug '06 – Dec '06	**-4.397**	**18**	**<0.001**	-1.347	14	0.199
Aug '06 – Dec '06 vs. Dec '06 - 2007	**5.905**	**18**	**<0.001**	**2.813**	**14**	**0.014**
Inward growth						
Jan '06 – Apr '06 vs. Apr '06 – Aug '06	**3.045**	**18**	**0.007**	-0.058	16	0.954
Apr '06 – Aug '06 vs. Aug '06 – Dec '06	**3.259**	**19**	**0.004**	1.330	16	0.202
Aug '06 – Dec '06 vs. Dec '06 – 2007	**2.780**	**19**	**0.012**	0.589	16	0.564
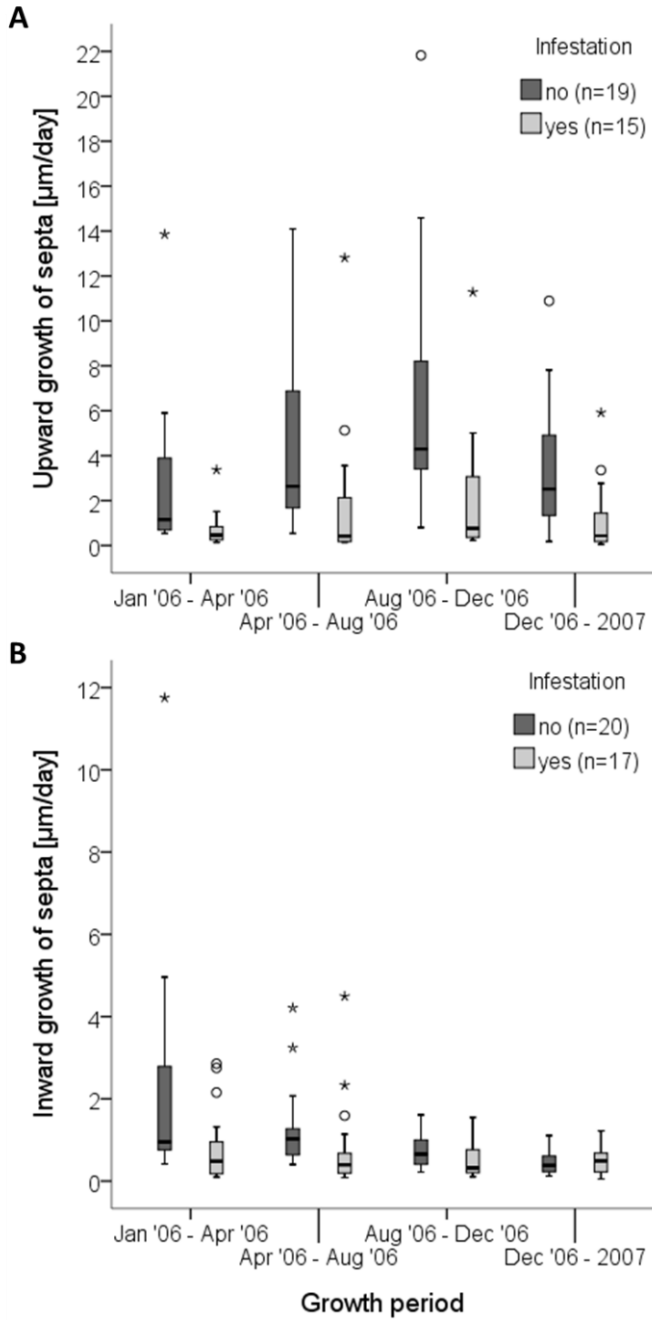
Figure 9: Seasonal variability in growth rates of *D. dianthus* at Fjord Comau, southern Chile; A: upward growth of septa; B: inward growth of septa; boxplot depicting median, interquartile range and non-outlier minimum and maximum, empty circles: mild outliers (more than 1.5 times the interquartile range), asterisks: extreme outliers (more than 3 times the interquartile range).

3.5 Gradual effect of infestation

Correlating growth rates with the total degree of infestation proved to be significant for USGR (Spearman's rank correlation, $\rho=-0.538$, $p<0.05$; figure 10A) as well as for ISGR (Spearman's rank correlation, $\rho=-0.447$, $p<0.05$; figure 10B). In both cases the relationship was negative showing a proportional decrease in ranked growth rates with an increasing rank of infestation. However, the correlation did only explain approx. 30% (USGR) and 20% (ISGR) of the variation in the data with a coefficient of correlation of $\rho^2=0.289$ and $\rho^2=0.200$, respectively.
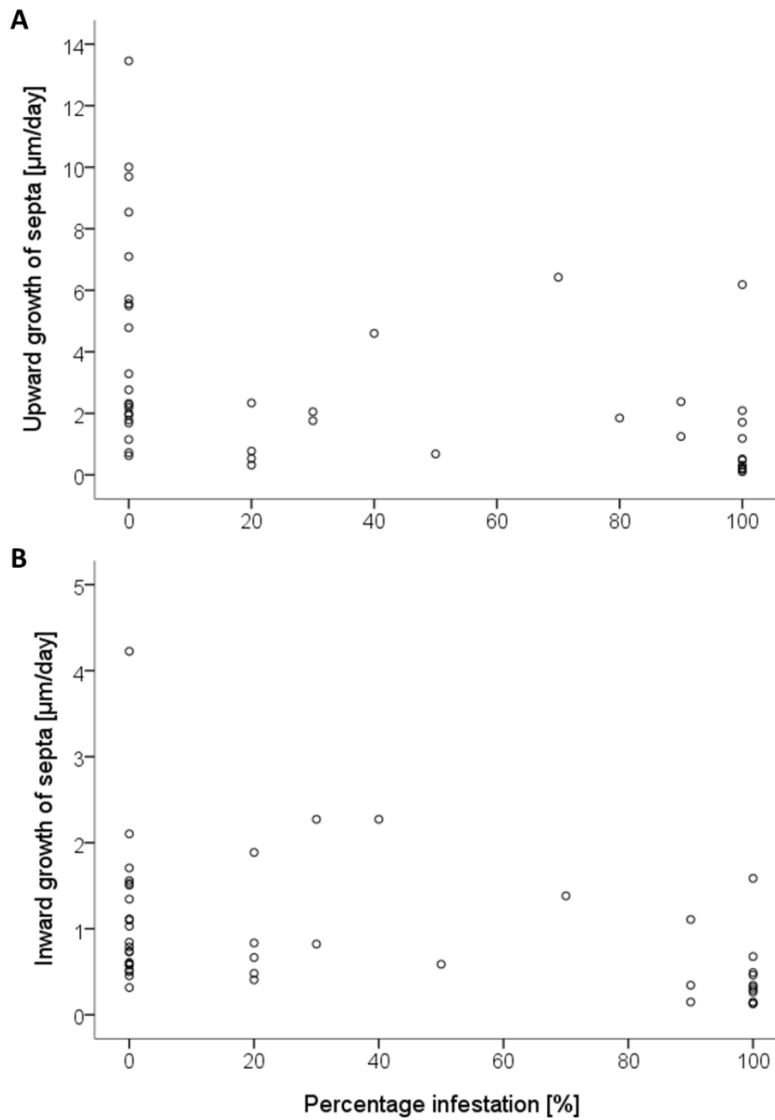

Figure 10: Correlation of the total degree of infestation and growth rates of *D. dianthus* at Fjord Comau, southern Chile; A: upward growth of septa (Spearman's rank correlation, $\rho=-0.538$, $p<0.05$), B: inward growth of septa (Spearman's rank correlation, $\rho=-0.447$, $p<0.05$).

3.6 Qualitative observations

Fluorescence microscopy

A qualitative comparison of two-dimensional images of septa between of an infested (A9; figure 11B) and a non-infested polyp (N0; figure 11A) using fluorescence (FM) and light field microscopy (LFM) revealed severe differences in skeletal characteristics. Most prominent were the numerous tunnelings of the endolithic algae that were visible in FM as well as LFM images (figure 11E+G). Endolith density appeared to have a strong periodicity with alternating areas of high and low density banding. In some cases these bands were fluorescent mimicking and obscuring skeletal growth bands of the coral polyp (figure 11I). This phenomenon considerably complicated the measuring of septal growth rates of infested polyps. Furthermore, septa of infested polyps appeared to be thicker than those of non-infested ones, especially in the apical area of the coral skeleton (figure 11E-H). This was observed in most of the polyps that were part of the experiment usually coinciding with slow growth rates. The front of Centers of Rapid Accretion was visible throughout the length of each septum as a brownish zigzagging line in LFM and a diffuse fluorescing band in FM images (figure 11E-I, K+L). It was located in the middle of the septum although it deviated to the edge in some cases (not shown). The line of the front of Centers of Rapid Accretion was not continuous as shown in figure 11F+H where the signal either weakened or disappeared. In infested polyps the identification of the front of Centers of Rapid Accretion was complicated by algal tunnelings (figure 11E, I, J).

Unlike the infested polyp A9 displayed in figure 11B that was infested by both endolithic species, polyps R2 and V1 were infested exclusively by either *O. queckettii* (R2; figure 11C) or *P. terebrans* (V1; figure 11D). Microscopic images of the theca and base of septa showed extensive tunneling of the endolithic algae in both polyps (figure 11I-L). In FM images tunneling of *O. queckettii* and *P. terebrans* differed slightly in color. *O. queckettii* fluoresced similar in intensity and color to that of the calcein-stained growth bands (figure 11I). Tunneling of *P. terebrans* had a more yellowish color (figure 11L). The dark structures visible in the background of LFM images were air bubbles trapped between the slide and the section as a result of a mishap in the preparation process (figure 11K+L).
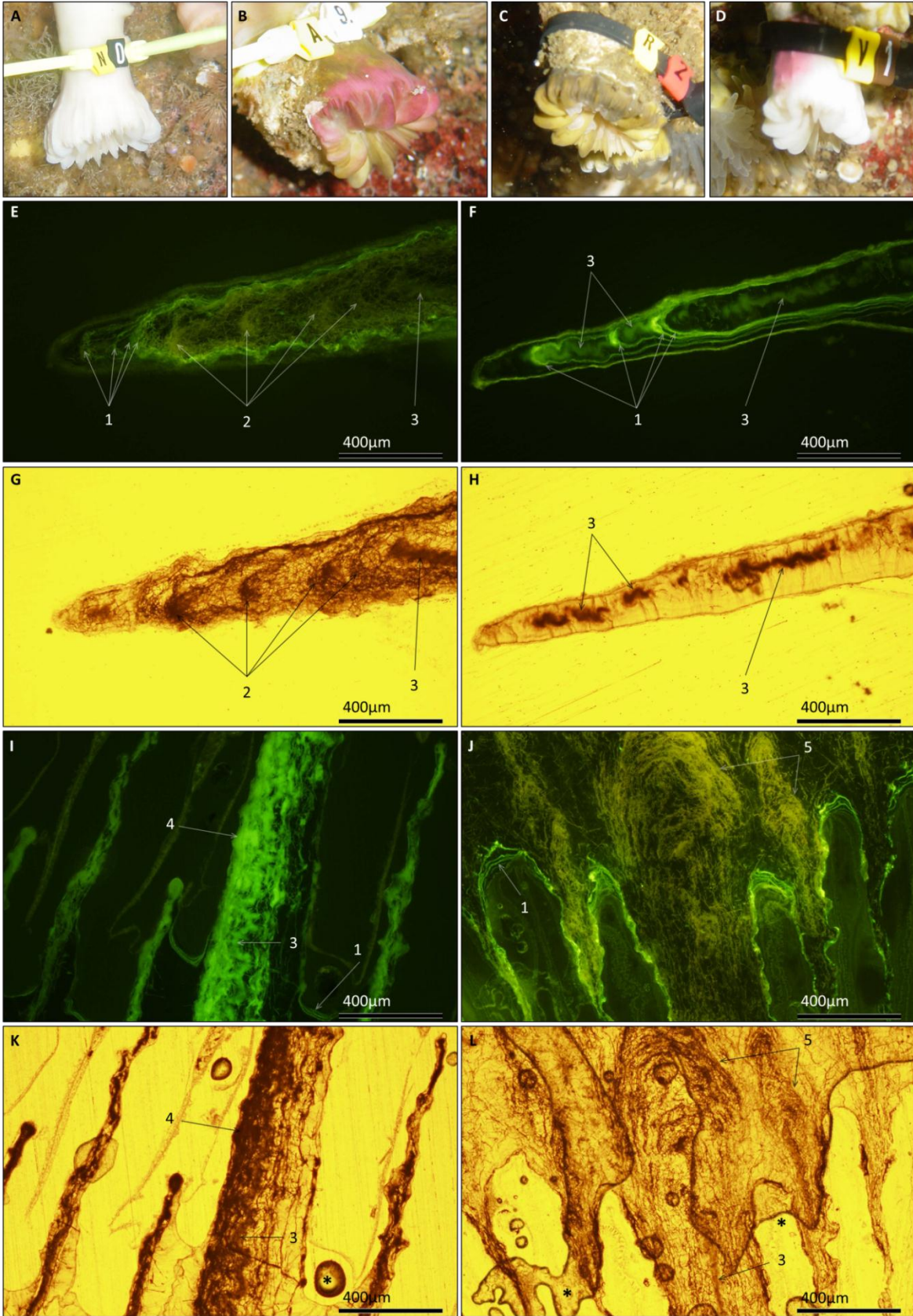
Figure 11: Fluorescence and light field microscopy images of *D. dianthus* at Fjord Comau, southern Chile; A-D: in-situ photographs of selected individuals; E+G: septum in a longitudinal section of infested polyp A9; F+H: septum in a longitudinal section of non-infested polyp N0; I+K: theca and base of septa in a transversal section of polyp R2 infested by *O. queckettii*; J+L: theca and base of septa in a transversal section of polyp V1 infested by *P. terebrans*; 1: calcein-stained growth bands of polyps, 2: high density bands of endolithic tunneling in polyp A9, 3: Rapid Accretion Front, 4: tunnelings of *O. queckettii* in polyp R2, 5: tunnelings of *P. terebrans* in polyp V1, asterisk: artifact by air bubbles trapped between slide and section.

A three-dimensional rendering of *D. dianthus* using individual FM images was not possible under the given conditions. Difficulties arose in the computer-based processing of the images. Image stacks could not be aligned and had varying pixel dimensions which prevented an analysis in AMIRA 5.4.1. Furthermore, the distance between FM images of 1.2mm would have been too large to give a reliable height resolution. However, the sectioning process of samples of *D. dianthus* did not allow for lesser values.

X-ray computed tomography

X-ray computed tomography produced grey-scale images of *D. dianthus* that allowed for an interpretation of differences in skeletal density. Lighter shaded areas in x-ray images corresponded to a higher skeletal density, whereas darker shaded areas pointed towards lesser density. From the four polyps that were x-rayed, one infested (to the right) and one non-infested polyp (to the left) are displayed here Figure 12A-E). Infested polyps had a visibly darker theca in x-ray images (figure 12.1+3) than non-infested ones (figure 12.2+4). Transversal slices further showed a thicker theca in infested polyps (figure 12E). The basal part of the skeleton of the infested polyp was partially destructed as indicated by a porous theca in the lower right-hand corner of figure 12A and discontinued septa in figure 12D.

The three-dimensional rendering of the two coral polyps illustrates the contrast in the shape of the coral skeleton between infested and non-infested polyps. As observed in the FM and LFM images, septa of infested polyps tended to be thicker. Furthermore septal growth of infested individuals seemed less regular. The apical arch of septa of infested polyps formed protrusions that correlated with areas of highest infestation and were absent in non-infested polyps (figure 12A+B). Some of these irregularities were already visible below the upper edge of the theca on the right-hand side of the infested polyp in figure 12E, where the basal part of the septa was considerably thicker than the distal part towards
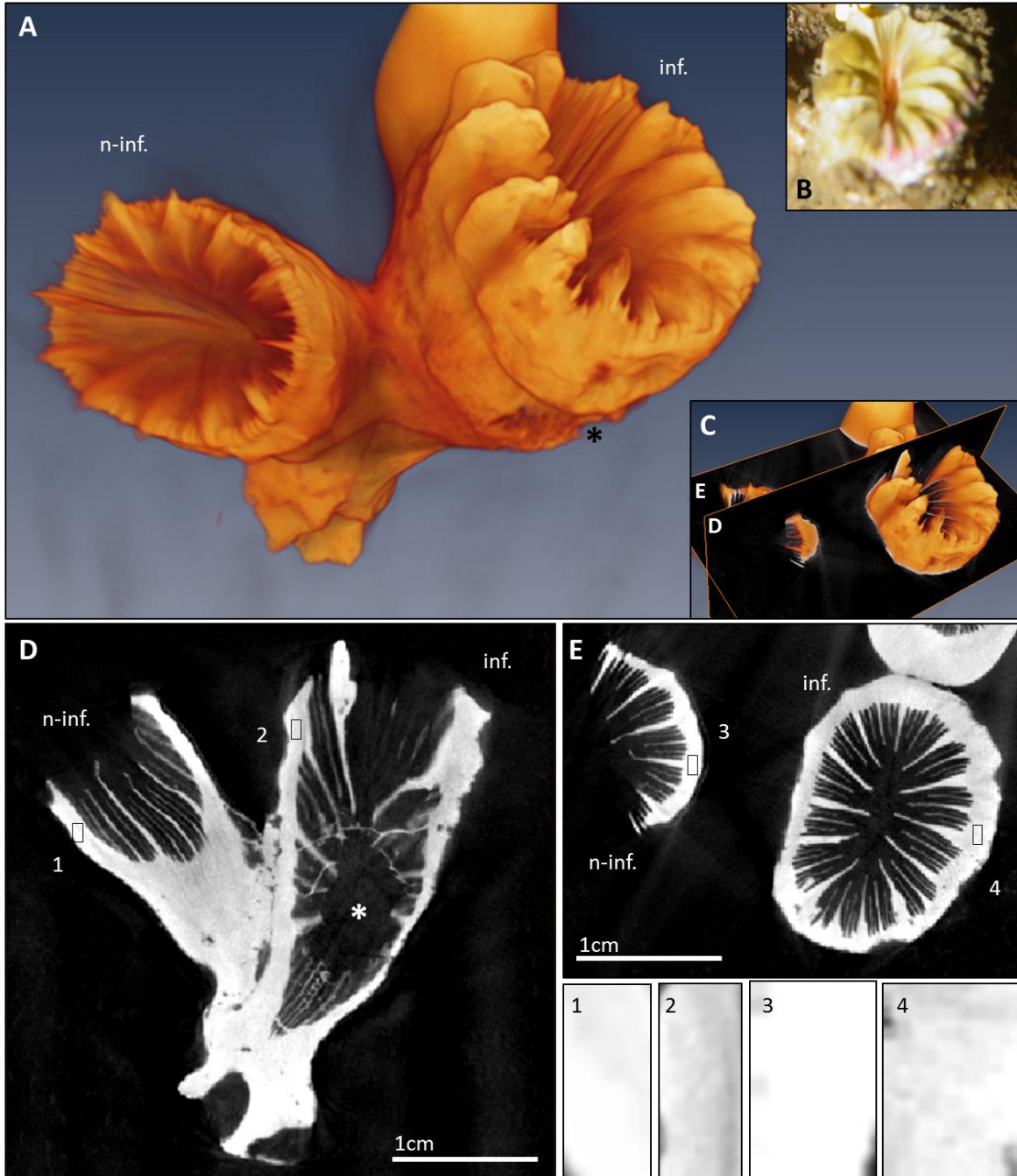
Figure 12: X-ray CT scan of *D. dianthus* collected at across Punta Huinay (XH), Fjord Comau, southern Chile; to the left of each image: non-infested polyp (n-inf.), to the right of each image: infested polyp (inf.); A: volume rendering, B: in-situ photograph of infested polyp, C: orientation and position of planar scans D (longitudinal) and E (transversal); 1-4 areas of the skeleton selected to compare grey-scale values (light-shaded: high density; dark-shaded: low density), asterisks: artifact caused by local destruction of the skeleton.

the center of the polyp. However, the polyp displayed in figure was an extreme example. Usually, infested polyps like the other one that was x-rayed and most of the ones used for the measurement of growth rates had less pronounced protrusions that were sometimes only visible by the increased thickness of septa. Thicker septa as well as thicker theca on the other hand were documented for most infested polyps. The three-dimensional rendering of the non-infested polyp gave the impression that septa only extended a short distance towards the center of the coral polyp (figure 12A). This was an artifact created by the insufficient resolution of the CT-images. The effect was less severe in the infested polyp where septa were usually thicker than the minimum resolution of images.

A short summary of the qualitative findings on skeletal characteristics of selecetd infested and non-infested specimens of *D. dianthus* are given in table 5.

Table 5: Summary of the qualitative observations on skeletal characteristics of infested and non-infested individuals of *D. dianthus* at Fjord Comau, southern Chile; comparison based on two non-infested and 4 infested specimens (2 infested by *O. quecketti* and *P. terebrans*; 1 infested by *O. queckettii*; 1 infested by *P. terebrans*); FM: fluorescence microscopy, LFM: light field microscopy.

	Non-infested	Infested
Endolithic tunnelings	- no	- yes - periodic change in density of algal filaments (most pronounced in septa) - visible in FM (varying shades of green) and LFM-images (brown)
Theca	- thinner	- thicker than in non-infested polyps
Septa	- thinner - more delicate	- thicker - displaying irregular growth in some cases (local protrusions of the apical arch of the septum) associated with heavy endolithic infestation
Front of Centers of Rapid Calcification	- visible in FM (green line) and LFM-images (brown line) - discontinuous	- visible in FM (green line) and LFM-images (brown line) - discontinuous - signal obscured by endolithic tunnelings
Calcein-stained growth bands	- clearly visible	- in some cases hard to identify - obscured by endolithic tunnelings fluorescing in similar color
Skeletal density	- higher, i.e. light shaded in x-ray images	- lower, i.e. darker shaded in x-ray images

4. DISCUSSION

4.1 Skeletal characteristics of *D. dianthus*

This study confirmed the presence of extensive tunnelings of both *O. queckettii* and *P. terebrans* in infested polyps of *D. dianthus* (Försterra et al., 2005). Endolithic tunnelings display a pronounced periodicity in filament density consistent with observations by Försterra and Häussermann (2008) in *D. dianthus* as well as by Risk et al. (1987) and Le Campion-Alsumard et al. (1995) in other scleractinian corals. Campion-Alsumard et al. (1995) suggested that filament density is influenced by algal seasonality and/or coral growth rates. Regarding the latter, high endolithic density is thereby corresponding to periods of slow coral growth and vice versa (Le Campion-Alsumard et al., 1995). Although it was not tested here, it is quite likely that a similar mechanism applies to *D. dianthus*. The distance between bands of high endolithic density appears to roughly match yearly growth rates of *D. dianthus*. Bands of highest filament density most likely correspond to coral growth in summer, when apical growth rates of *D. dianthus* are slowest growth (see section 4.4 Seasonality of growth rates) and algal growth is expected to be highest.

Along the middle of septa and thecae of *D. dianthus* the meandering front of Centers of Rapid Accretion was visible in fluorescence microscopy (FM) images as a green and in light field microscopy (LFM) images as a brown band as described by Stolarski (2003) and Cuif and Dauphin (2005a, b). Acridine orange staining was so far used for FM observations of the front of Centers of Rapid Accretion (Gautret et al., 2000; Stolarski, 2003; Cuif and Dauphin, 2005b). In this study the front of Centers of Rapid Accretion was also fluorescent in calcein-stained polyps. The reason for this phenomenon is still unknown.

Infested individuals of *D. dianthus* display a fluorescence that is associated with the tunnelings of the endolithic algae. This fluorescence differed in color between polyps probably depending on the infesting species. In some cases endolithic tunnelings fluoresced in the same color as the calcein-stained growth bands. The cause of this fluorescence can only be speculated about. It is possible that the endolithic algae deposit calcium carbonate in form of calcite (MacIntyre and Towe, 1976) which would be stained by calcein as well as aragonite deposited by the coral polyp (Rowley and Mackinnon, 1995). Calcein may also have been trapped in endolithic tunnelings after staining. A third

explanation involves a possible autofluorescence of dead organic material of endolithic algae in the tunnelings.

4.2 Effect of endolithic algae on the growth of *D. dianthus*

Unlike previously suggested (Cairns et al., 2005; Försterra et al., 2005; Försterra and Häussermann, 2008) the association between *D. dianthus* and its endolithic algae has characteristics of a parasitic relationship. The reduced growth rates of infested polyps are a strong indicator that the presence of endolithic algae is negatively affecting the fitness of the coral host. Instead of promoting calcification as hypothesized by e.g. supplying energy, endolithic algae are rather posing an extra cost to the coral host. The amount of energy resources available to a coral polyp is limited. Once the costs of ensuring the polyp's survival and health are covered, the surplus is allocated to growth and reproduction. If the health of the polyp is compromised by diseases or parasitic infection, energy resources are subtracted from reproduction or growth. Given the evidence provided in this study, this cost may lead to (I) an increase in the amount of energy necessary for calcification or (II) a decrease in the energy allocated to calcification, resulting in a reduction of growth rates.

Infested polyps of *D. dianthus* display extensive endolithic tunnelings of *O. queckettii* as well as *P. terebrans*. The role of these two endolithic species, especially *O. queckettii*, as major bioeroders has so far been thought to be restricted to the skeleton of dead corals (Schneider and Le Campion-Alsumard, 1999; Tribollet, 2007, 2008). In living corals only a minor effect on skeletal bulk density has been attributed to their boring activity (Highsmith, 1981). However, judging by the extensive endolithic tunnelings observed in *D. dianthus*, it is very likely that the ultrastructure of infested polyps may be closer to that of an inwardly eroded dead skeleton (Tribollet, 2008) than previously anticipated. Hollow endolithic tunnelings would severely reduce skeletal density.

Heavily infested areas of the skeleton show thicker skeletal structures, i.e. thecae and septa, which were previously thought to indicate enhanced calcification (Försterra et al., 2005). However, these areas appear to correspond to regions of reduced skeletal density as documented by x-ray CT images and slow polyp growth contradicting the assumption of increased calcification. Thicker skeletal structures might represent the attempt of the coral

polyp to counteract the weakening of the skeleton by the boring activity of the endoliths and to stabilize infested areas. This may require energy resources of the coral polyp to be allocated to the maintenance of skeletal intactness rather than the vertical growth of the polyp.

Several polyps of *D. dianthus* developed local protrusions and tumor-like deformations of skeletal structures in septal areas that were heavily infested by endolithic algae. These irregularities in skeletal growth may be a more extreme form of the thickening of skeletal structures. Skeletal deformations have been described in other coral species as a response to parasites and are known to negatively affect fitness by increasing mortality and reducing coral growth and reproduction (Beuck et al., 2007; Work et al., 2008; McClanahan et al., 2009; Aeby et al., 2011). Polyps of the cold-water coral *Lophelia pertusa* exhibit swollen corralites when infested by boring sponges (Beuck et al., 2007). In *Porites* spp. skeletal anomalies might initiated by boring organisms such as fungi (McClanahan et al., 2009). It is possible that the irregular growth of infested *D. dianthus* is a further indicator of a parasitic relationship between the coral host and its endolithic algae.

One of the major arguments for a symbiosis between *D. dianthus* and its endolithic algae has been the close spatial proximity of the polyp tissue and the endolith (Cairns et al., 2005; Försterra et al., 2005; Försterra and Häussermann, 2008) that has also been observed in other coral species in studies on *O. queckettii* (Gutner-Hoch and Fine, 2011). The spatial proximity requires the endolith to facilitate any exchange with the seawater through the coral tissue – a process that was suspected to have the potential for a mutually beneficial transfer of substances (Försterra and Häussermann, 2008). Ongoing studies on the transfer of metabolites in *D. dianthus* document either a very low or no flow of substances toward from the endolith to the coral host (Försterra et al., 2012). In the last case the substance flow may also have been too low to be detected (Jantzen, 2012, pers. comm.). However, the reduction of growth rates does not indicate a positive effect on the energy budget of *D. dianthus* resulting from this process. It is possible that the endolith is receiving metabolites from the coral host (Titlyanov et al., 2008), e.g. benefitting from the uptake of excretion products of the polyp. This mechanism would explain why endolithic algae are so closely associated with the coral tissue.

The severity of the negative effect of endolithic algae on growth rates of *D. dianthus* appears to increase with the degree of infestation. This correlation was based on the

analysis of in-situ photographs that were used to estimate the percentage surface area of the polyp colored by endolithic algae and septal growth rates. Despite the mathematical significance of the correlation, it did not explain a large amount of the variation in the data. The measurement of the degree of infestation is subject to several biases and might not very reliable. The photographs were a two-dimensional representation of the original polyp and only half of the polyp was visible in each of them. Endolithic coloring on the remote side of the camera could not be considered in the analysis. Estimates of the degree of infestation were mostly based on the percentage skeletal area colored by endolithic algae alone. The density of endolithic filaments was largely neglected since it was hard to evaluate this parameter using photographs. Furthermore, the correlation includes hardly any data on polyps with an intermediate degree of infestation. The majority were either non-infested or so heavily infested that their whole skeleton was colored by endoliths. A better way to investigate the gradual effect of infestation might be regression analysis given that enough data is available on polyps with intermediate infestation.

4.3 Effect of location along the fjord on growth rates of *D. dianthus*

Additional to the overall decrease in growth rates associated with endolithic infestation, this study suggests a difference in this effect between sampling sites. Growth rates of non-infested polyps were much higher at the mouth of the fjord suggesting more favorable conditions at this location. The influence of Pacific Ocean increases towards the mouth of fjord (Pickard, 1971) and might provide a better environment than the conditions at mid-fjord sites. Data on temperature, salinity and pH-levels indicates a significant change in these parameters along the course of the fjord in the depth where *D. dianthus* was sampled (Baumgarten, 2012, not publ.). However, previous work on the tolerance of *D. dianthus* to fluctuations in pH-levels did not show a severe effect of this parameter (Jantzen et al., 2011). Temperature and salinity are known to be paramount in determining the distribution of *D. dianthus* (Försterra and Häussermann, 2003; Cairns et al., 2005; Försterra et al., 2005) and may also affect skeletal growth rates. On the other hand, the differences in temperature and salinity between the outer and mid-fjord sites appear to be within the tolerance range of *D. dianthus*. Other factors that may influence polyp growth

are current velocities (Sokol, 2011) and food availability (Naumann et al., 2011). However, current velocities at Fjord Comau not seem to vary between the outer and mid-fjord (Sokol, 2011). No data is as yet available on food availability.

By contrast, it is peculiar that growth rates of infested individuals do not seem to be affected by changes in oceanographic conditions. They display similar growth rates at the mouth of the fjord as well as at mid-fjord sites. If conditions at mid-fjord sites were generally less favorable than at the mouth of the fjord, this should affect infested and non-infested polyp alike. The exceptionally high growth rates of non-infested polyps at the mouth of the fjord should also be interpreted with caution. Unlike the data on growth rates at mid-fjord sites, only one site (Isla Liliguapi) was chosen to represent the outer fjord. The high growth rates at this site may be unique to Isla Liliguapi and not transferrable to other sites at the mouth of the fjord.

Unlike the data on inward growth rates, measurements of the upward growth of septa allowed for the analysis using the original two-way ANOVA design. The two factors were defined as 'infestation' and 'site' with 'site' referring to the five different sampling sites of the experiment. The results did not vary noticeably from the ones described above where Isla Liliguapi at the outer fjord was compared to the pooled data from the four mid-fjord sites. They confirmed the significant main effect of infestation and further revealed a significant interaction between infestation and site (appendix B, table 9). This interaction between infestation and site was not to be expected under the hypothesis that the negative effect of infestation is ubiquitous. To explain the different severity of algal infestation at different sites, the possibility of a sampling bias should not be neglected. Coral polyps were chosen according to how well a bag could be fitted around them for staining. Differences in the accessibility of coral polyps between sites might have affected the selection process and resulted in biased growth rate estimates.

Previous work on growth rates of *D. dianthus* used the outward thickening of the theca as measurement of growth (Kupprat, 2011). It was restricted to the mid-fjord sampling sites and did not detect any differences in growth rates between infested and non-infested individuals (Kupprat, 2011). The current study did not reveal statistically significant differences in septal growth rates between non-infested polyps and infested individuals at mid-fjord sites either, although median septal growth rates, especially of the apical extension, of non-infested individuals were still higher. It raises the question if the effect of

endolithic infestation on the growth of *D. dianthus* is as severe as it seems. However, Whether the insignificance of this result is due to an insufficient sample size, a sampling bias, an error in the measuring process, a high natural variation of growth rates or the fact that infestation does not affect growth rates at mid-fjord sites still needs to be determined.

4.4 Seasonality of growth rates

The upward extension of septa of infested as well as non-infested *D. dianthus* displayed a pronounced seasonality with minimum growth rates in January to April and a maximum growth in August to December. Although this pattern was only observed in one year, it is very likely that it is not caused by coincidence. The growth rates reported for the period from December 2006 to the coral harvest 2007 approx. matched the mean growth between January and August 2006 indicating that the seasonality is a recurring pattern.

It was expected that growth rates of *D. dianthus* were positively related with temperature. Highest temperatures usually correspond to the most productive season of the year with the highest supply of food (Iriarte et al., 2007), which would provide energy for calcification. The pattern observed in this study, however, is not consistent with yearly fluctuations in temperature. Slowest growth rates were reported for the period of highest temperatures while maximum growth occurred at and just after the yearly temperature minimum (figure 13). Although the data on temperature was not collected during this study but in 2011 (Baumgarten, 2012, not publ.), there should be no severe deviations from this pattern.

It has been suggested that marine organisms in cold-water regions use the season of the year which offers the highest food supply for reproduction rather than skeletal growth (Waller, 2005; Waller and Tyler, 2005). The trade-off between reproduction and growth would result in the reduced growth rates in summer. A similar pattern has already been observed in Antarctic brachiopods (Peck et al., 1997, 2000). This explanation could be applied to *D. dianthus*. However, data on the reproductive cycle of *D. dianthus* is not yet available.
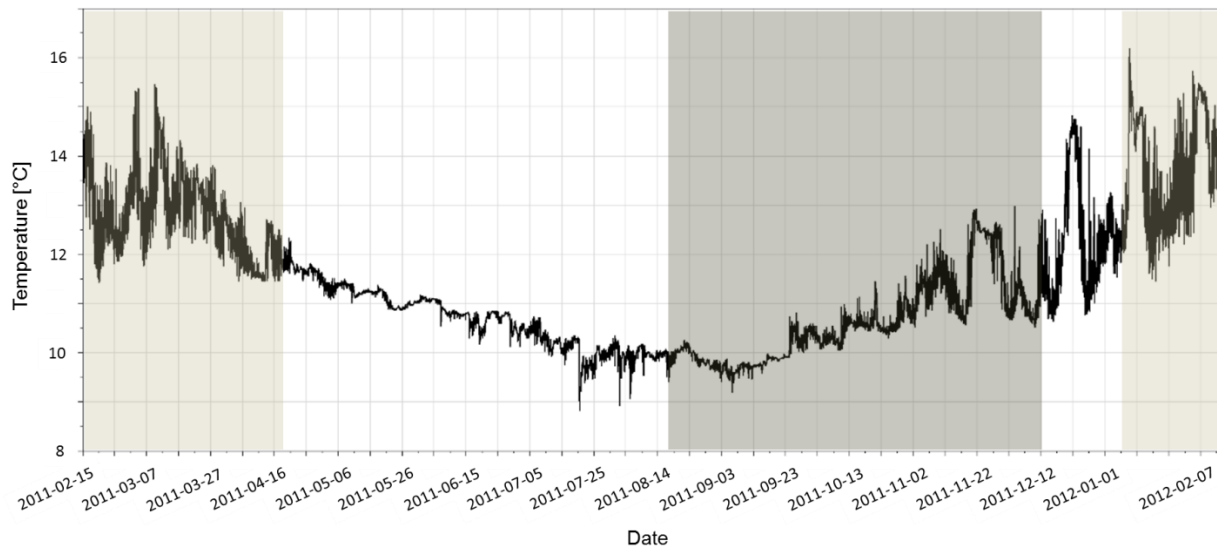
Figure 13: Seasonal fluctuations in temperature at Isla Liliguapi, southern Chile, from Febr. 2011 – 2012 (Baumgarten, 2012, not publ.); light shaded area corresponding to period of minimum upward septal growth of *D. dianthus*, dark shaded area corresponding to period of maximum upward septal growth of *D. dianthus*.

4.5 Evaluation of methodology

During the course of this study, several aspects of the sampling design and methodology were discovered that could be improved in future studies. Overall, calcein staining proved to be a useful technique to document the growth of *D. dianthus*. However, the tagging process should be optimized. After the one and a half years of the experiment when polyps were stained in-situ, the retrieval rate of tagged polyps was less than 65%. To account for this loss future tagging studies should consider tagging more polyps or modifying the tagging technique.

A further loss of samples occurred during the embedding process. The main problems were the consistency of the embedding medium and the air trapped between skeletal structures, mostly septa, during embedding. Embedding of insufficiently dried polyps usually resulted in a in a very sticky consistency of the epoxy resin which prevented further processing of the samples. In a few cases the consistency of the epoxy resin was rubber-like instead of solid most likely caused by a wrong ratio of resin and hardener. Of the two embedding resins used in this study, araldite 2020 gave the better results. However, embedding under pressure and increased temperatures to reduce the hardening

time did not prove advantageous. Fissures in the embedding medium occurred during hardening, probably promoted by trapped air bubbles. For further studies araldite 2020 should be used as en embedding medium. The hardening of embedded samples should not be forced. Adding a solvent to lower the viscosity of the embedding medium might prevent the trapping of air between skeletal structures ensuring the complete integrity of the sample during sectioning.

In this study two measurements were taken from each specimen: upward (USGR) and inward septal growth rates (ISGR). USGR correspond to the apical, i.e. longitudinal, growth of the polyp whereas ISGR measured linear septal extension towards the centre of the polyp. The linear extension of septa in this direction is limited by morphological constraints, i.e. the restricted space in the centre of the polyp. The rate of inward septal growth is most likely depending to a large degree on how much further this extension is morphologically possible. A continuous reduction of ISGR that was revealed by measurements on seasonality was therefore to be expected. A seasonal pattern similar to that of USGR (see section 4.4 Seasonality of growth rates) could no longer be identified. To compensate for these morphological constraints the sectioning plane should have been adjusted for each growth period. Since the space in the center of the polyp is getting more limited with each growth period, several sectioning planes should have been employed, each a little bit closer to the apical part of the polyp than the last (figure 14). However, since USGR appear to give reliable data on coral growth, further studies should rather exclude inward growth rates than to spend additional time on the adjustment of sectioning planes.

Dec '06 – 2007
Aug '06 – Dec '06
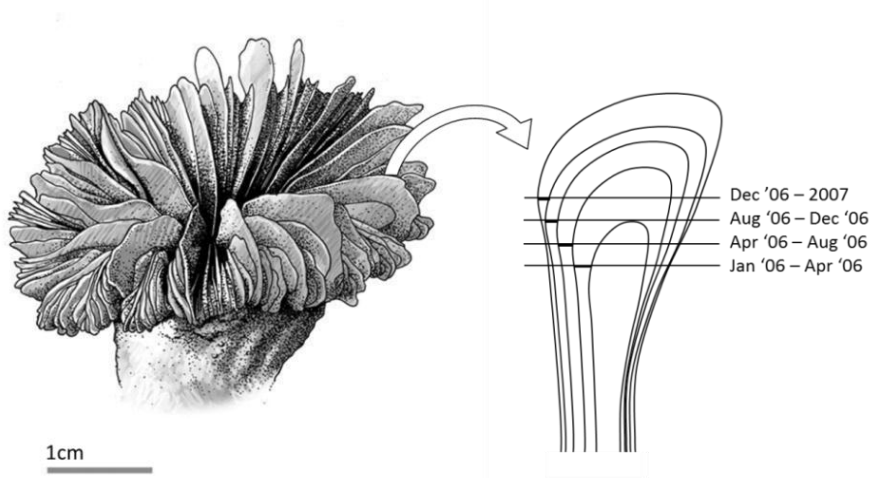Apr '06 – Aug '06
Jan '06 – Apr '06

1cm

Figure 14: Schematic of *D. dianthus* depicting the adjustment of the sectioning plane to measure seasonal variability of inward septal growth; modified after Roberts et al. (2009).

Measurements of ISGR were further biased in other ways. First, the sectioning plane to measure ISGR was set at approx. 4mm below the upper edge of the theca (see section 2.3 Sclerology). Depending on polyp morphology and age, ISGR in this plane were subject to the constraint of limited space in the center of the polyp to varying degrees. The large range of values of ISGR may be an indicator of this bias. Furthermore, in very slow growing polyps septal growth was sometimes so minimal that individual growth bands could not be clearly identified. These septa were not measured. Therefore, estimates of ISGR most likely constitute overestimates of the actual growth of the polyp. It might further have led to an underestimate of the negative effect of infestation on growth rate, since mostly growth rates of infested polyps would have been subject to the bias.

One concern during the analysis was a potentially inverse relationship between polyp age and growth rates. It has been shown in *Balanophyllia europaea* and *Lophelia pertusa* that younger polyps grow faster than older ones (Goffredo et al., 2004; Maier et al., 2009). This pattern has also been observed in *D. dianthus* (Jantzen, 2012, pers. comm.). Since the infestation with endolithic algae is only occurring after the retraction of the coal tissue from the base of the polyp, infested polyps tend to be older than non-infested individuals (Lazier et al., 1999; Försterra and Häussermann, 2003, 2008). This factor could have given a false-positive effect of infestation. Infested polyps would not have been growing slower due to algal infestation but because of their age. However, using polyp diameter as proxy for age did not reveal an inverse relationship. In selected cases this relationship was even positive, underestimating the effect of infestation rather than overestimating it. Furthermore a decrease of growth rates with increasing polyp age is only documented for young individuals (Jantzen, 2012, pers. comm.). The size range of polyps selected for this study, however, was that of older individuals. Although polyp diameter is predominantly determined by age, it is also suspected to be subject to other factors than (Försterra et al., 2005) and might not necessarily give an unbiased estimate of polyp age. Still, to fully resolve the matter further studies should consider measuring polyp length as an additional proxy for age and including it as a covariate in the analysis of the effect of infestation.

The foremost goal of future research on the association of *D. dianthus* with endolithic algae should be an increase in the spatial scope of the current study. So far, the analysis has been restricted to fjord Comau, southern Chile, where 47 polyps were measured. Expanding the experiment should contribute greatly to resolving any discrepancies

revealed in this study. To base the assessment of the effect of endolithic algae on *D. dianthus* not solely on growth rates other techniques should be employed such as the analysis of substance flow between the endolith and the coral tissue or skeletal densitometry. X-ray CT scans are known to provide reliable data on skeletal density of corals (Bosscher, 1993) and have already been employed to collect preliminary data on differences in skeletal density between two infested and non-infested individuals of *D. dianthus*. A large scale densitometry of *D. dianthus* might confirm the suspicion that skeletal density is severely reduced in infested polyps.

4.6 Conclusion

Despite increasing research on *D. dianthus* the ecology of this cold-water coral is still poorly understood. This study investigated growth patterns of *D. dianthus* to document seasonal fluctuations in growth rates and assess the effect of association with endolithic algae on growth performance. Contrary to previous suggestions the relationship between *D. dianthus* and its associated endolithic algae appears to be parasitic leading to reduced growth rates of infested individuals. This is further supported by first observations on skeletal density which seems to be negatively affected by algal infestation. The seasonal pattern of apical growth rates of *D. dianthus* is preserved in infested individuals. However, the relationship of *D. dianthus* and its endolithic algae still remains controversial. Experiments on the transfer of metabolites detected a low substance flow from the endolith to the coral host (Försterra et al., 2012). To solve these controversies and to agree on a final classification of the relationship between *D. dianthus* and its endolithic algae further research is necessary. Future studies will concentrate on skeletal densitometry of *D. dianthus* and metabolic links between the coral host and the endolith.

ACKNOWLEDGEMENTS

REFERENCES

Adkins, J.F., Henderson, G.M., Wang, S.-L., O'Shea, S., Mokadem, F., 2004. Growth rates of the deep-sea scleractinia *Desmophyllum cristagalli* and *Enallopsammia rostrata*. Earth and Planetary Science Letters 227, 481–490.

Aeby, G.S., Williams, G.J., Franklin, E.C., Haapkyla, J., Harvell, C.D., Neale, S., Page, C.A., Raymundo, L., Vargas-Ángel, B., Willis, B.L., Work, T.M., Davy, S.K., 2011. Growth anomalies on the coral genera *Acropora* and *Porites* are strongly associated with host density and human population size across the Indo-Pacific. PLoS ONE 6, e16887.

Al-Horani, F.A., Al-Moghrabi, S.M., de Beer, D., 2003. The mechanism of calcification and its relation to photosynthesis and respiration in the scleractinian coral *Galaxea fascicularis*. Marine Biology 142, 419–426.

Allemand, D., Ferrier-Pagès, C., Furla, P., Houlbrèque, F., Puverel, S., Reynaud, S., Tambutté, É., Tambutté, S., Zoccola, D., 2004. Biomineralisation in reef-building corals: from molecular mechanisms to environmental control. Comptes Rendus Palevol 3, 453–467.

Allemand, D., Tambutté, É., Zoccola, D., Tambutté, S., 2011. Coral calcification, cells to reefs, in: Coral Reefs: An Ecosystem in Transition. pp. 119–150.

Baumgarten, S., 2012. Oceanography of Fjord Comau. (data not published, 2 April 2012).

Beuck, L., Vertino, A., Stepina, E., Karolczak, M., Pfannkuche, O., 2007. Skeletal response of *Lophelia pertusa* (Scleractinia) to bioeroding sponge infestation visualised with micro-computed tomography. Facies 53, 157–176.

Bosscher, H., 1993. Computerized tomography and skeletal density of coral skeletons. Coral Reefs 12, 97–103.

Brahmi, C., Meibom, A., Smith, D.C., Stolarski, J., Auzoux-Bordenave, S., Nouet, J., Doumenc, D., Djediat, C., Domart-Coulon, I., 2009. Skeletal growth, ultrastructure and composition of the azooxanthellate scleractinian coral *Balanophyllia regia*. Coral Reefs 29, 175–189.

Buhl-Mortensen, L., Mortensen, P.B., 2004. Symbiosis in deep-water corals. Symbiosis 37, 33–61.

Cairns, S.D., Häussermann, V., Försterra, G., 2005. A review of the Scleractinia (Cnidaria: Anthozoa) of Chile, with the description of two new species. Zootaxa 1018, 15–46.

Le Campion-Alsumard, T., Golubic, S., Hutchings, P., 1995. Microbial endoliths in skeletons of live and dead corals: *Porites lobata* (Moorea, French Polynesia). Marine Ecology Progress Series 117, 149–157.

Carreiro-Silva, M., McClanahan, T., Kiene, W., 2009. Effects of inorganic nutrients and organic matter on microbial euendolithic community composition and microbioerosion rates. Marine Ecology Progress Series 392, 1–15.

Chalker, B., Taylor, D., 1975. Light-enhanced calcification, and the role of oxidative phosphorylation in calcification of the coral *Acropora cervicornis*. Proceedings of the Royal Society of London. Series B, Biological Sciences 323–331.

Cuif, J.P., Dauphin, Y., 1998. Microstructural and physico-chemical characterization of "centers of calcification" in septa of some recent scleractinian corals. Paläontologische Zeitschrift 72, 257–269.

Cuif, J.P., Dauphin, Y., 2005a. The Environment Recording Unit in coral skeletons – a synthesis of structural and chemical evidences for a biochemically driven, stepping-growth process in fibres. Biogeosciences 2, 61–73.

Cuif, J.P., Dauphin, Y., 2005b. The two-step mode of growth in the scleractinian coral skeletons from the micrometre to the overall scale. Journal of structural biology 150, 319–331.

Endesa Fundacion San Ignacio del Huinay. Oceanographic conditions of Fjord Comau. Available at http://www.fundacionhuinay.cl/oceanographic.html (Accessed 29 March 2012).

Fine, M., Loya, Y., 2002. Endolithic algae: an alternative source of photoassimilates during coral bleaching. Proceedings of the Royal Society B: Biological Sciences 269, 1205–1210.

Fork, D., Larkum, A., 1989. Light harvesting in the green alga *Ostreobium* sp., a coral symbiont adapted to extreme shade. Marine Biology 103, 381–385.

Försterra, G., Beuck, L., Häussermann, V., Freiwald, A., 2005. Shallow-water *Desmophyllum dianthus* (Scleractinia) from Chile: characteristics of the biocoenoses, the bioeroding community, heterotrophic interactions and (paleo)-bathymetric implications, in: Cold-water Corals and Ecosystems. pp. 937–977.

Försterra, G., Häussermann, V., 2003. First report on large scleractinian (Cnidaria: Anthozoa) accumulations in cold-temperate shallow water of south Chilean fjords. Zoologische Verhandelingen 117–128.

Försterra, G., Häussermann, V., 2008. Unusual symbiotic relationships between microendolithic phototrophic organisms and azooxanthellate cold-water corals from Chilean fjords. Marine Ecology Progress Series 370, 121–125.

Försterra, G.; Häussermann, V.; Mayr, C.; Jantzen, C.; Hassenrück, C., 2012. Low pH and the role of endolithic algae in cold-water corals. International Symposium on Deep-Sea Corals, Amsterdam, Netherlands, April 2-6, 2012.

Freitag, J., 2012. AWI-ICE CT. (personal communication, 3 April 2012).

Furla, P., Galgani, I., Durand, I., Allemand, D., 2000. Sources and mechanisms of inorganic carbon transport for coral calcification and photosynthesis. Journal of Experimental Biology 203, 3445–3457.

Gattuso, J.P., Allemand, D., Frankignoulle, M., 1999. Photosynthesis and calcification at cellular, organismal and community levels in coral reefs: a review on interactions and control by carbonate chemistry. American Zoologist 39, 160–183.

Gautret, P., Cuif, J.P., Stolarski, J., 2000. Organic components of the skeleton of scleractinian corals-evidence from in situ acridine orange staining. Acta Palaeontologica Polonica 45, 107–118.

Goffredo, S., Mattioli, G., Zaccanti, F., 2004. Growth and population dynamics model of the Mediterranean solitary coral *Balanophyllia europaea* (Scleractinia, Dendrophylliidae). Coral Reefs 23, 433–443.

Gutner-Hoch, E., Fine, M., 2011. Genotypic diversity and distribution of *Ostreobium quekettii* within scleractinian corals. Coral Reefs 30, 643–650.

Highsmith, R.C., 1981. Lime-boring algae in hermatypic coral skeletons. Journal of Experimental Marine Biology and Ecology 55, 267–281.

Iriarte, J., González, H., Liu, K., Rivas, C., Valenzuela, C., 2007. Spatial and temporal variability of chlorophyll and primary productivity in surface waters of southern Chile (41.5-43 S). Estuarine, Coastal and Shelf Science 74, 471–480.

Jantzen, C., Häussermann, V., Försterra, G., Laudien, J., Richter, C., 2011. The cold water coral *Desmophyllum dianthus* grows along a pH gradient in the Comau Fjord (Patagonia, Chile). YOUMARES 2.0, Bremerhaven, Germany, 7 September 2011 - 9 September 2011.

Jantzen, C., 2012. Ecology of *Desmophyllum dianthus*. (personal communication, 18 April 2012).

Kanwisher, J.W., Wainwright, S.A., 1967. Oxygen balance in some reef corals. The Biological Bulletin 133, 378–390.

Kupprat, F., 2011. The relationship between the presence of microendolithic phototrophic organisms and the growth of the cold-water coral *Desmophyllum dianthus*. Bachelor thesis University of Cologne.

Lazier, A.M.Y.V., Smith, J.E., Risk, M.J., Schwarcz, H.P., 1999. The skeletal structure of *Desmophyllum cristagalli*: the use of deep-water corals in sclerochronology. Lethaia 32, 119–130.

MacIntyre, I.G., Towe, K.M., 1976. Skeletal calcite in living scleractinian corals: microboring fillings, not primary skeletal deposits. Science 193, 701.

Maier, C., Hegeman, J., Weinbauer, M.G., Gattuso, J.P., others, 2009. Calcification of the cold-water coral *Lophelia pertusa* under ambient and reduced pH. Biogeosciences 6, 1671–1680.

Marschal, C., Garrabou, J., Harmelin, J.G., Pichon, M., 2004. A new method for measuring growth and age in the precious red coral *Corallium rubrum* (L.). Coral Reefs 23, 423–432.

Marshall, A.T., Clode, P., 2004. Calcification rate and the effect of temperature in a zooxanthellate and an azooxanthellate scleractinian reef coral. Coral Reefs 23.

McClanahan, T.R., Weil, E., Maina, J., 2009. Strong relationship between coral bleaching and growth anomalies in massive *Porites*. Global Change Biology 15, 1804–1816.

McConnaughey, T.A., Whelan, J.F., 1997. Calcification generates protons for nutrient and bicarbonate uptake. Earth-Science Reviews 42, 95–117.

Miller, K.J., Rowden, A.A., Williams, A., Häussermann, V., 2011. Out of their depth? Isolated deep populations of the cosmopolitan coral *Desmophyllum dianthus* may be highly vulnerable to environmental change. PLoS ONE 6, e19004.

Moya, A., Tambutté, S., Tambutté, E., Zoccola, D., Caminiti, N., Allemand, D., 2006. Study of calcification during a daily cycle of the coral *Stylophora pistillata*: implications for 'light-enhanced calcification'. Journal of Experimental Biology 209, 3413.

Naumann, M.S., Orejas, C., Wild, C., Ferrier-Pagès, C., 2011. First evidence for zooplankton feeding sustaining key physiological processes in a scleractinian cold-water coral. Journal of Experimental Biology 214, 3570–3576.

Nothdurft, L.D., Webb, G.E., 2006. Microstructure of common reef-building coral genera *Acropora*, *Pocillopora*, *Goniastrea* and *Porites*: constraints on spatial resolution in geochemical sampling. Facies 53, 1–26.

Odum, H.T., Odum, E.P., 1955. Trophic structure and productivity of a windward coral reef community on Eniwetok Atoll. Ecological Monographs 25, 291–320.

Peck, L.S., Brockington, S., Brey, T., 1997. Growth and metabolism in the Antarctic brachiopod *Liothyrella uva*. Philosophical Transactions of the Royal Society of London. Series B: Biological Sciences 352, 851–858.

Peck, L.S., Colman, J.G., Murray, A.W.A., 2000. Growth and tissue mass cycles in the infaunal bivalve *Yoldia eightsi* at Signy Island, Antarctica. Polar Biology 23, 420–428.

Pickard, G.L., 1971. Some physical oceanographic features of inlets of Chile. Journal of the Fisheries Research Board of Canada 28, 1077–1106.

Pytkowicz, R.M., 1973. Calcium carbonate retention in supersaturated seawater. American Journal of Science 273, 515–522.

Risk, M., Heikoop, J., Snow, M., Beukens, R., 2002. Lifespans and growth patterns of two deep-sea corals: Primnoa resedaeformis and *Desmophyllum cristagalli*. Hydrobiologia 471, 125–131.

Rotjan, R.D., Lewis, S.M., 2005. Selective predation by parrotfishes on the reef coral *Porites astreoides*. Marine Ecology Progress Series 305, 193–201.

Rowley, R.J., Mackinnon, D.I., 1995. Use of the fluorescent marker calcein in biomineralisation studies of brachiopods and other marine organisms. Bulletin de l'Institut oceanographique, Monaco 14, 111–120.

Schlichter, D., Berglund, O., Backe, C., Eklöv, A., Järnmark, C., Persson, A., 1995. Transfer of photoassimilates from endolithic algae to coral tissue. Naturwissenschaften 82, 559–561.

Schlichter, D., Kampmann, H., Conrady, S., 1997. Trophic potential and photoecology of endolithic algae living within coral skeletons. Marine Ecology 18, 299–317.

Schneider, J., Le Campion-Alsumard, T., 1999. Construction and destruction of carbonates by marine and freshwater cyanobacteria. European Journal of Phycology 34, 417–426.

Shashar, N., Banaszak, A.T., Lesser, M.P., Amrami, D., 1997. Coral endolithic algae: Life in a protected environment. Pacific Science 51, 167–173.

Shashar, N., Stambler, N., 1992. Endolithic algae within corals-life in an extreme environment. Journal of Experimental Marine Biology and Ecology 163, 277–286.

Sokol, S., 2011. The influence of heterotrophy and flow on calcification of the cold-water coral *Desmophyllum dianthus*. Diploma thesis Christian–Albrechts–University of Kiel.

Stolarski, J., 2003. Three-dimensional micro- and nanostructural characteristics of the scleractinian coral skeleton: A biocalcification proxy. Acta Palaeontologica Polonica 48, 497–530.

Tambutte, E., Tambutte, S., Segonds, N., Zoccola, D., Venn, A., Erez, J., Allemand, D., 2011. Calcein labelling and electrophysiology: insights on coral tissue permeability and calcification. Proceedings of the Royal Society B: Biological Sciences 279, 19–27.

Tambutté, S., Holcomb, M., Ferrier-Pagès, C., Reynaud, S., Tambutté, É., Zoccola, D., Allemand, D., 2011. Coral biomineralization: From the gene to the environment. Journal of Experimental Marine Biology and Ecology.

Tambutté, S., Tambutté, E., Zoccola, D., Caminiti, N., Lotto, S., Moya, A., Allemand, D., Adkins, J., 2006. Characterization and role of carbonic anhydrase in the calcification process of the azooxanthellate coral *Tubastrea aurea*. Marine Biology 151, 71–83.

Thresher, R.E., Adkins, J., Thiagarajan, N., 2011. Modal analysis of the deep-water solitary scleractinian, *Desmophyllum dianthus*, on SW Pacific seamounts: inferred recruitment periodicity, growth, and mortality rates. Coral Reefs 30, 1063–1070.

Titlyanov, E.A., Kiyashko, S.I., Titlyanova, T.V., Kalita, T.L., Raven, J.A., 2008. $\delta13C$ and $\delta15N$ values in reef corals *Porites lutea* and *P. cylindrica* and in their epilithic and endolithic algae. Marine Biology 155, 353–361.

Tribollet, A., 2007. Dissolution of dead corals by euendolithic microorganisms across the northern Great Barrier Reef (Australia). Microbial Ecology 55, 569–580.

Tribollet, A., 2008. The boring microflora in modern coral reef ecosystems: a review of its roles. Current Developments in Bioerosion 67–94.

Waller, R., 2005. Deep-water Scleractinia (Cnidaria: Anthozoa): current knowledge of reproductive processes, in: Cold-Water Corals and Ecosystems. pp. 691–700.

Waller, R.G., Tyler, P.A., 2005. The reproductive biology of two deep-water, reef-building scleractinians from the NE Atlantic Ocean. Coral Reefs 24, 514–522.

Weber, J.N., White, E.W., Weber, P.H., 1975. Correlation of density banding in reef coral skeletons with environmental parameters: the basis for interpretation of chronological records preserved in the coralla of corals. Paleobiology 137–149.

Willenz, P., 2011. Epoxy-embedded samples of *Desmopyllum dianthus*. (personal communication, 7 November 2011).

Work, T., Aeby, G., Coles, S., 2008. Distribution and morphology of growth anomalies in Acropora from the Indo-Pacific. Diseases of Aquatic Organisms 78, 255–264.

Yonge, C.M., 1931. The significance of the relationship between corals and zooxanthellae. Nature 128, 309–311.

Yonge, C.M., Nicholls, A.G., 1931. Studies on the physiology of corals. V. On the relationship between corals and zooxanthellae. Scient. Rep. Gt. Barrier Reef Exped. 1, 177–211.

Appendix A – Data tables

Table 6: Upward septal growth rates of *D. dianthus* at Fjord Comau, southern Chile; n/a: missing value; not found: polyp not found at the staining event at the end of the respective growth period – growth rates of following growth period recorded over both growth periods; LI: Isla Liliguapi, PG: Punta Gruesa, PH: Punta Huinay, SW: steep wall after Punta Llonco, XH: across Punta Huinay.

Site	Ind.no	Growth rate [µm/day]					Diameter [mm]
		Jan '06 – Apr '06	Apr '06 – Aug '06	Aug '06 – Dec '06	Dec '06 – 2007	mean over seasons	
LI	(+)0	0.32	0.18	0.46	0.28	0.31	18.99
LI	(+)1	2.29	1.37	not found	1.47	1.71	22.49
LI	(+)2	0.22	0.14	0.24	0.05	0.16	17.90
LI	(+)6	0.26	0.16	0.28	0.17	0.22	22.39
LI	(+)9	1.52	1.48	2.01	3.35	2.09	22.35
LI	(0)0	5.90	11.91	8.42	2.14	7.09	n/a
LI	(0)1	n/a	4.52	21.82	6.79	9.70	15.24
LI	(0)3	5.15	2.91	4.14	7.81	5.57	16.39
LI	(0)4	n/a	11.53	11.74	3.03	8.54	16.21
LI	(0)5	n/a	9.37	13.46	7.20	10.01	16.39
LI	(0)7	13.86	14.09	14.59	10.89	13.46	21.53
PG	R2	0.82	0.93	0.46	2.77	1.25	17.29
PG	R5	0.14	0.15	1.22	0.40	0.48	18.03
PG	R6	0.38	0.40	0.32	0.19	0.32	15.34
PG	T4	1.43	1.93	3.96	2.30	2.27	10.80
PG	T6	1.18	1.88	3.38	2.87	2.33	11.35
PG	T7	0.68	0.54	1.47	0.19	0.72	13.00
PG	T9	0.71	1.69	5.74	2.93	2.76	13.28
PH	L6	0.55	0.33	0.81	0.43	0.53	17.57
PH	LV1	0.10	0.12	not found	0.07	0.10	17.99
PH	S03	3.96	7.52	8.00	2.52	5.50	12.92
PH	S07	0.54	1.54	not found	3.29	1.79	13.50
PH	S1	1.68	1.00	not found	3.48	2.05	19.59
PH	S20	3.65	8.65	not found	2.06	4.78	15.51

Table 6 continued.

Site	Ind.no	Growth rate [μm/day]					Diameter [mm]
		Jan '06 – Apr '06	Apr '06 – Aug '06	Aug '06 – Dec '06	Dec '06 – 2007	mean over seasons	
SW	A1	3.37	5.13	11.28	5.91	6.42	16.75
SW	A3	0.34	2.37	not found	0.85	1.18	15.63
SW	A5	not found	2.66	9.30	6.60	6.19	15.77
SW	A6	0.84	3.56	4.12	0.99	2.38	n/a
SW	A7	0.90	2.50	not found	1.89	1.76	20.11
SW	A8	0.25	0.19	0.27	0.10	0.20	19.28
SW	A9	0.37	0.41	0.76	0.52	0.52	17.85
SW	N0	1.13	1.66	3.43	1.55	1.94	17.00
SW	N1	n/a	12.81	4.24	1.89	4.60	18.50
SW	N2	0.54	0.76	2.15	1.16	1.15	18.75
SW	N7	3.82	6.23	7.68	6.87	5.72	17.48
XH	E1	1.85	3.44	not found	0.27	1.85	18.29
XH	E3	not found	0.33	0.95	0.76	0.68	15.05
XH	E8	1.02	1.49	0.41	0.16	0.77	16.31
XH	V+6	0.62	0.89	0.80	0.18	0.62	14.45
XH	V0	1.21	1.75	4.30	1.49	2.19	13.81
XH	V1	0.76	2.77	5.01	0.81	2.34	12.89
XH	V4	1.02	4.02	5.15	2.96	3.29	14.50
XH	V5	0.59	1.67	3.38	1.11	1.69	12.85
XH	V8	0.76	2.64	3.43	1.19	2.01	14.05

Table 7: Inward septal growth rates of D. dianthus at Fjord Comau, southern Chile; n/a: missing value; not found: polyp not found at the staining event at the end of the respective growth period – growth rates of the following growth period recorded over both growth periods; LI: Isla Liliguapi, PG: Punta Gruesa, PH: Punta Huinay, SW: steep wall after Punta Llonco, XH: across Punta Huinay.

Site	Ind.no	Growth rate [µm/day]					Diameter [mm]
		Jan '06 – Apr '06	Apr '06 – Aug '06	Aug '06 – Dec '06	Dec '06 – 2007	mean over seasons	
LI	(+)0	0.13	0.16	0.16	0.07	0.13	18.99
LI	(+)1	1.11	0.84	not found	0.08	0.68	22.49
LI	(+)2	0.25	0.62	0.28	0.23	0.34	17.90
LI	(+)6	0.10	0.13	0.25	0.05	0.13	22.39
LI	(+)9	0.81	0.30	0.15	0.58	0.46	22.35
LI	(0)0	4.43	1.13	0.40	0.28	1.56	n/a
LI	(0)1	4.96	2.07	1.23	0.15	2.10	15.24
LI	(0)3	2.88	1.31	0.82	1.11	1.53	16.39
LI	(0)4	3.42	0.99	0.75	0.68	1.34	16.21
LI	(0)5	n/a	3.24	1.61	0.27	1.71	16.39
LI	(0)7	11.75	4.21	1.05	0.44	4.22	21.53
PG	R1	0.13	0.21	0.15	0.10	0.15	17.70
PG	R2	0.49	0.20	0.20	0.49	0.34	17.29
PG	R5	0.11	0.16	0.30	0.71	0.32	18.03
PG	R6	0.20	0.68	0.37	0.68	0.48	15.34
PG	T4	0.52	0.84	0.42	0.58	0.59	10.80
PG	T6	0.83	0.86	0.66	0.57	0.73	11.35
PG	T7	0.42	0.40	0.32	0.12	0.32	13.00
PG	T9	0.75	1.23	0.22	0.76	0.74	13.28
PH	L6	0.95	1.14	0.70	0.55	0.83	17.57
PH	LV1	0.62	0.77	not found	0.08	0.49	17.99
PH	S03	0.51	0.66	0.44	0.73	0.58	12.92
PH	S07	0.54	0.16	not found	0.66	0.45	13.50
PH	S1	0.69	0.43	not found	1.35	0.82	19.59
PH	S20	1.60	0.88	not found	0.86	1.11	15.51

Table 7 continued.

| Site | Ind.no | Growth rate [µm/day] | | | | | Diameter [mm] |
		Jan '06 – Apr '06	Apr '06 – Aug '06	Aug '06 – Dec '06	Dec '06 – 2007	mean over seasons	
SW	A1	1.32	1.59	1.55	1.08	1.38	16.75
SW	A3	0.16	0.29	not found	0.34	0.26	15.63
SW	A5	not found	1.06	1.72	1.99	1.59	15.77
SW	A6	2.15	0.37	0.83	1.07	1.11	n/a
SW	A7	4.27	1.97	not found	0.57	2.27	20.11
SW	A8	0.18	0.40	0.32	0.26	0.29	19.28
SW	A9	0.18	0.08	0.11	0.22	0.15	17.85
SW	N0	0.77	0.60	0.65	0.41	0.61	17.00
SW	N1	2.86	4.49	1.17	0.57	2.27	18.50
SW	N2	0.48	0.56	0.94	0.36	0.58	18.75
SW	N6	2.75	2.33	1.25	1.22	1.89	19.60
SW	N7	2.70	1.17	1.52	0.63	1.51	17.48
XH	E3	not found	0.83	0.58	0.35	0.59	15.05
XH	E8	0.70	0.53	0.34	0.06	0.41	16.31
XH	V+6	0.95	0.62	1.40	0.18	0.79	14.45
XH	V0	2.38	1.06	0.66	0.30	1.10	13.81
XH	V1	0.76	0.67	0.76	0.46	0.66	12.89
XH	V2	0.86	0.50	0.56	0.17	0.52	15.74
XH	V4	2.18	1.40	0.25	0.28	1.03	14.50
XH	V5	0.77	0.74	0.30	0.18	0.50	12.85
XH	V8	1.31	1.11	0.49	0.46	0.84	14.05

Table 8: Infestation status of *D. dianthus* collected at Fjord Comau, southern Chile; Infestation by *O. queckettii*, *P. terebrans* and total infestation by endolithic algae given as percentage surface area of the coral skeleton colored by endolithic algae; LI: Isla Liliguapi, PG: Punta Gruesa, PH: Punta Huinay, SW: steep wall after Punta Llonco, XH: across Punta Huinay.

Site	Ind.no	*O. queckettii* [%]	*P. terebrans* [%]	Endoliths (total) [%]	Infestation
LI	(+)0	90	10	100	yes
LI	(+)1	100	0	100	yes
LI	(+)2	100	0	100	yes
LI	(+)6	90	10	100	yes
LI	(+)9	100	0	100	yes
LI	(0)0	0	0	0	no
LI	(0)1	0	0	0	no
LI	(0)3	0	0	0	no
LI	(0)4	0	0	0	no
LI	(0)5	0	0	0	no
LI	(0)7	0	0	0	no
PG	R1	90	0	90	yes
PG	R2	90	0	90	yes
PG	R5	100	0	100	yes
PG	R6	0	20	20	yes
PG	T4	0	0	0	no
PG	T6	0	0	0	no
PG	T7	0	0	0	no
PG	T9	0	0	0	no
PH	L6	20	0	20	yes
PH	LV1	100	0	100	yes
PH	S03	0	0	0	no
PH	S07	0	0	0	no
PH	S1	0	30	30	yes
PH	S20	0	0	0	no

Table 8 continued.

Site	Ind.no	*O. queckettii* [%]	*P. terebrans* [%]	Endoliths (total) [%]	Infestation
SW	A1	70	0	70	yes
SW	A3	100	0	100	yes
SW	A5	100	0	100	yes
SW	A6	90	0	90	yes
SW	A7	0	30	30	yes
SW	A8	90	10	100	yes
SW	A9	50	50	100	yes
SW	N0	0	0	0	no
SW	N1	40	0	40	yes
SW	N2	0	0	0	no
SW	N6	20	0	20	yes
SW	N7	0	0	0	no
XH	E1	80	0	80	yes
XH	E3	50	0	50	yes
XH	E8	20	0	20	yes
XH	V+6	0	0	0	no
XH	V0	0	0	0	no
XH	V1	0	20	20	yes
XH	V2	0	0	0	no
XH	V4	0	0	0	no
XH	V5	0	0	0	no
XH	V8	0	0	0	no

Table 9: Results of the ANOVAs to determine differences in diameter and upward septal growth rates of *D. dianthus* at Fjord Comau, southern Chile; significant results in bold script; tests conducted on ln-transformed growth rates.

Variable	Source of variation	Effect	SS type III	df	MS	F	p
Diameter							
	Site	**fixed**	**130.118**	**4**	**32.530**	**11.205**	**<0.001**
	Infestation	**fixed**	**87.875**	**1**	**87.875**	**30.269**	**<0.001**
	Infestation*Site	**fixed**	**34.855**	**4**	**8.714**	**3.002**	**0.031**
	Error		101.609	35	2.903		
		R²	0.717				
Upward growth rates of septa							
	Infestation	**fixed**	**17.243**	**1**	**17.243**	**20.713**	**<0.001**
	Site	fixed	3.130	4	0.782	0.940	0.453
	Infestation*Site	**fixed**	**11.360**	**4**	**2.840**	**3.412**	**0.019**
	Error		28.304	34	0.832		
		R²	0.544				

Table 10: Correlation of septal growth rates and polyp diameter of *D. dianthus* at Fjord Comau, southern Chile; significant results in bold script; tests conducted on ln-transformed growth rates.

	Non-infested		Infested	
	Pearson's R	p	Pearson's R	p
Upward growth	**0.445**	**0.049**	-0.117	0.605
Jan '06 – Apr '06	0.500	0.057	-0.174	0.570
Apr '06 – Aug '06	0.407	0.094	-0.297	0.303
Aug '06 – Dec '06	0.335	0.175	-0.260	0.370
Dec '06 – 2007	0.402	0.099	-0.007	0.981
Inward growth	**0.626**	**0.002**	-0.069	0.755
Jan '06 – Apr '06	**0.585**	**0.011**	-0.131	0.629
Apr '06 – Aug '06	0.433	0.064	-0.230	0.391
Aug '06 – Dec '06	**0.575**	**0.010**	-0.310	0.243
Dec '06 – 2007	0.057	0.818	-0.200	0.457

Table 11: RM-MANOVA to test for seasonality of septal growth rates of *D. dianthus* at Fjord Comau, southern Chile; significant results in bold script; test conducted on ln-transformed growth rates.

	Source of variation	SS type VI	df	MS	F	p
Upward septal growth						
univariate	**Infestation**	**54.556**	**1**	**54.556**	**14.449**	**<0.001**
	Error	105.725	28	3.776		
multivariate	**TIME**	**10.318**	**3**	**3.439**	**12.150**	**<0.001**
	TIME*infestation	0.853	3	0.284	1.004	0.395
	Error	23.779	84	0.283		
Inward septal growth						
univariate	**Infestation**	**13.435**	**1**	**13.435**	**6.678**	**0.014**
	Error	68.397	34	2.012		
multivariate	**TIME**	**14.068**	**3**	**4.689**	**13.795**	**<0.001**
	TIME*infestation	**5.312**	**3**	**1.771**	**5.209**	**0.002**
	Error	34.672	102	0.340		

Appendix C – List of figures

Appendix D – List of tables

EIDESTATTLICHE ERKLÄRUNG

Hiermit versichere ich, dass ich diese Arbeit selbstständig verfasst und keine anderen als die angegeben Quellen und Hilfsmittel benutzt habe. Außerdem versichere ich, dass ich die allgemeinen Prinzipien wissenschaftlicher Arbeit und Veröffentlichung, wie sie in den Leitlinien guter wissenschaftlicher Praxis der Carl von Ossietzky Universität festgelegt sind, befolgt habe.

Unterschrift: